PEOPLE'S DEMOCRATIC REPUBLIC OF ALGERIA

Ministry of Higher Education and Scientific Research

Serial Number: ...../2024

University Kasdi Merbah Ouargla
Faculty of Hydrocarbons, Renewable Energies, Earth and Universe Sciences
Department of Earth and Universe Sciences

THESIS

To obtain the Master's Degree

Option: Hydrocarbon Geology

Subject:

Building a Precise 1D Mechanical Earth Model and its application in hydraulic fracturing and drilling operation using Techlog and Excel Case study HTF-19

Presented by: GHACHOU Zineb

Defended on: 29/06/2024

Members of the jury:

President: Mr. Beleksier Med Saleh	**M.C.A**	**U.K.M. OUARGLA**
Examiner: Mr.Hamza Laouini	**M.A.A**	**U.K.M. OUARGLA**
Supervisor: Mr. Medjani Fethi	**M.C.A**	**U.K.M. OUARGLA**

Academic Year: 2023/2024

Dedications

To my dear parents, a source of tenderness and affection, as a token of gratitude and obedience from their daughter who has always prayed for their health and happiness.

To my dear brothers and sisters, Mohmed, Abderrahman, Messaoud, and sisters, Houiada Fatima and Ihssane ,always attentive and whose respect and pride in me have inspired me to succeed.

To my lifelong friend and beloved Amani

Acknowledgements

I would like to express my deepest gratitude to those who have supported and guided me throughout the completion of this master's degree project.

First and foremost, to my parents, for their unwavering love, support, and belief in me. Your encouragement has been my foundation and inspiration.

I extend my sincere gratitude to Dr. Medjani Fathi, my professor and supervisor, for accepting to be my encadron.

Special thanks to Kamel Mekerri from SH rock mechanics services for his kindness, insightful feedback, and dedicated time, which greatly contributed to this work.

My heartfelt thanks to BABKEUR Med Nasr Eddine, DATA Engineer at NESR, for his relentless support and efforts.

I am grateful to the SH-DP engineers, especially Mohcen BOUFAGHES for providing the theme, data, and documentation crucial for my project, and to Kacem Bahedi for his thorough reviews and valuable feedback, ensuring the project's accuracy. Additionally, I appreciate Kamel Karboua for his assistance in securing the internship, a pivotal experience in my academic journey. I also extend warm thanks to Imane Fantazi, Hanan, and Sehame for their kindness and support during my internship.

Finally, I want to thank everyone else who supported me throughout this journey. Your encouragement and belief in me have been a source of strength and motivation.

Thank you all for being part of this journey and helping me achieve this milestone.

Zineb Ghachou

Contents

List of figures ..... **A**
List of Tables ..... **B**
General Introduction **1**
Chapter I: Generalities **3**
I. Tight reservoir concepts 3
I.1- Conventional and Unconventional reservoirs 3
I.2- Petrophysical characteristics of tight reservoirs 4
I.3- Difficulties related to tight reservoirs. 4
I.4- Techniques for exploiting tight reservoirs 5
II. Pressure. 7
II.1- Pressure Concepts 7
II.2- Types of pressure 7
III. Fracturing. 12
III.1- Hydraulic fracturing. 12
III.2- Constraints related to fracturing. 13
III.3 Selection of zones for fracturing in Tight reservoirs 14
III.4 Contribution of Geomechanics in Hydraulic Fracturing 15
I. Presentation of Hassi Tarfa Field (HTF) 16
I.1 Geographic location 17
I.2 Field history 17
I.3 Lithostratigraphic Overview 18
II.4 Structural aspect 21
II.5. Petroleum system 24
III. Case study Well HTF-19. 27
III.1 Geographical location 27
III.2 The geological framework 27
III.3 Structural aspect 28
III.4 Petrophysical Characteristics 28
Chapter III: Methods and Materials **30**
I. Mechanical Earth Model (MEM) 1D Definition 30
II. Components of the 1D Geomechanical Model 30
II.2 Elastic Parameters of Rocks 32
II.3 Rock Strength Parameters 35
II.4 Pore Pressure 36
II.5 Fracture Pressure 36
III. Steps for Developing a Geomechanical Model 36
IV. Methods for Determining the Minimum Stress Zone 37
I V.1 Calculation of Elastic Properties of Rocks 40
IV.2 Calculation of Pore Pressure and Stresses 42
V. Identification of the Fracture Zone 47
VI. Wellbore Stability 47
VI.1 Factors Influencing Wellbore Stability 47

VI.2 Maintaining Wellbore Stability 48
VII. Mud Weight 48
VIII. Software Used 50
VIII.1 Microsoft Excel 50
VIII.2 Techlog Software 50
IX. Conclusion 51
Chapter III: **53**
Practical part **53**
I. Introduction 53
II. Study Objective 53
III. Mechanical Earth Model 1D Workflow 53
III.1 Main data used and data Audit 54
IV. Geomechanics model construction (MEM 1D) 55
IV.1 Rock Mechanical Properties Computation 55
III.3 Mechanical Elastic Properties 55
III.4 Rock Strength Computation 59
IV. In-situ Stresses and Pore Pressure 61
IV.1 Vertical Stress and Pore Pressure 61
IV.2 Horizontal stress directions 63
IV.3 Horizontal stress magnitudes 63
V. Wellbore Stability 65
V.1 Rock Failure Criteria 65
V.2 Mud Weight Window 66
VI. Conclusions and recommendations 69
Chapter IV: Results and Discussion **72**
I. Introduction 72
II. Stress interpretation 72
II.1 Vertical Stress Analysis 74
III. Mud Weight 74
III.1 Recommended Mud Weight for Drilling a New Well: 77
IV. Conclusion 77
General Conclusion **78**
References **79**

List of figures

Figure1: Conventional reservoir (Encyclopaedia Britannica, Inc 2012)	**3**
Figure 2: Unconventional reservoir (Oil and Gas Institute of Monastir)	**4**
Figure 3: Hydraulic fracturing in an oil well	**5**
Figure 4: Architecture of a Short Radius well.	**7**
Figure 5: Hydrostatic Pressure in a Column	**8**
Figure 6: Factors of Overburden Pressure (Vertical)	**9**
Figure 7: Pressure Relationship as a Function of Depth	**11**
Figure 8: Conceptual diagram of hydraulic fracturing (Total)	**13**
Figure 9: Schematic representation of stresses	**14**
Figure 10: The concept of the 1D geomechanical model (1D MEM)	**15**
Figure 11: Location of the Hassi Terfa Field.	**17**
Figure 12: Stratigraphic Column of the Hassi Tarfa Region.	**21**
Figure 13: Structural map of Quartzite Hamra top in Hassi Tarfa field	**23**
Figure 14: Isobath map at the top of the Hamra Quartzites	**24**
Figure 15: Geological cross-section NW-SE.	**26**
Figure 16: Positioning plan of Well HTF-19	**27**
Figure 17: Technical data sheet of well HTF-19	**28**
Figure 18: Principal Stresses	**31**
Figure 19: Fault models according to the stress regime	**32**
Figure 20: Deformation along a stress axis of a cylinder.	**33**
Figure 21: Lateral and axial deformations resulting from compression	**34**
Figure 22: Mechanical Earth Model Workflow	**36**
Figure 23: Modeling P and S Wave Propagation in Rocks	**39**
Figure 24: Stress Distribution around a Wellbore in the Rock Formation	**44**
Figure 25: Fracture opening relative to horizontal stresses.	**46**
Figure 26 Determination of horizontal stresses according to induced fractures and wellbore ovalization	**46**
Figure 27: Interface of Microsoft Excel Software	**50**
Figure 28: Interface of Techlog Software	**50**
Figure 29: The Mechanical Earth Model Workflow	**54**
Figure 30: Static versus dynamic Young's modulus and Poisson's ratio derived from core test data of well HTF-19	**56**
Figure 31: Rock elastic properties from logs and cores for well HTF-19.	**58**
Figure 32: UCS versus static Young's modulus and compressional slowness from HTF-19 and HTF 10 core test data	**59**
Figure 33: Location of Wells HTF19 and HTF10 in the HTF Field	**59**
Figure 34: Rock Strength parameters from logs and cores for HTF-19	**61**
Figure 35: Overburden/vertical stress calculation for HTF-19 (Using Excel)	**62**

.

Figure 36: Distribution of horizontal stresses around a vertical wellbore and associated failures.	**63**
Figure 37: In-situ Stress profiles for HTF-1 9 with calibration data from injection test.	**64**
Figure 38: HTF19 MEM 1D Stress Profile Log (By Excel)	**65**
Figure 39: Wellbore Stability limits	**66**
Figure 40: Wellbore stability analysis results for HTF-19	**67**
Figure 41: Wellbore stability analysis results for HTF-19 | (Using Excel)	**68**
Figure 42: Stress Regime	**73**
Figure 43: HTF19 MEM 1D Stress Profile Log (Using Excel)	**73**
Figure 44: Wellbore stability analysis results for HTF-19	**75**
Figure 45: Comparing Wellbore Diameter to Bit Size: Stability Assessment	**76**
Figure 46: Mud window for new well in HTF region	**77**

List of Tables

Table 1: Some Examples of Young's Modulus.	**33**
Table 2: Some examples of Poisson's ratio	**34**
Table 3: Data Required for Building MEM	**37**

General Introduction

In the realm of petroleum geology, understanding and modeling the subsurface mechanical behavior is crucial for optimizing extraction processes. The Mechanical Earth Model (MEM) stands as a pivotal tool in this endeavor, providing a comprehensive framework that integrates geological, geophysical, and engineering data to characterize the subsurface's mechanical properties. This study focuses on constructing a precise 1D MEM and explores its application in both drilling and hydraulic fracturing operations, utilizing advanced software tools such as Techlog and Excel. Through a detailed case study of the HTF-19 well, we aim to demonstrate how MEM can enhance the efficiency and safety of hydrocarbon extraction in tight reservoirs.

Tight reservoirs, characterized by their low permeability and complex stress conditions, pose significant challenges in hydrocarbon extraction. Conventional methods often fall short in these environments, necessitating advanced techniques such as hydraulic fracturing to improve fluid flow and sophisticated drilling strategies to ensure wellbore stability and efficiency. The MEM plays a crucial role in this context by providing insights into the stress distribution and mechanical properties of the reservoir rock, which are essential for designing effective drilling and fracturing strategies.

Drilling operations in tight reservoirs require a thorough understanding of the subsurface pressures and rock mechanics to prevent issues such as wellbore collapse, lost circulation, and differential sticking. The MEM helps in predicting the stress regimes and pore pressure distribution, allowing for optimized mud weight and casing programs. This ensures that the wellbore remains stable throughout the drilling process, minimizing non-productive time and reducing operational risks.

This work begins by outlining the fundamental concepts of tight reservoirs, including their petrophysical characteristics and the difficulties they present. We then delve into the construction of the MEM, detailing the methodologies and data integration processes involved. Finally, we apply the MEM to the HTF-19 well, illustrating its practical benefits in optimizing both drilling and hydraulic fracturing operations.

Chapter I: Generalities

Chapter I: Generalities

I. Tight reservoir concepts

Whether conventional or unconventional hydrocarbons, their origin is the same: the transformation of various organic materials (algae, plants, animals...) deposited in source rock, through increasing temperature and pressure during burial over geological time. Conventional reservoirs can produce economical volumes of oil and gas without requiring extensive stimulation treatments or recovery processes, which is not the case for unconventional reservoirs.

I.1- Conventional and Unconventional reservoirs

I.1.1. Conventional reservoirs

In this case, the hydrocarbons thus formed follow a classic geological trajectory; they migrate towards a porous and permeable rock (the reservoir) where they will be trapped (structural or stratigraphic traps). We have deposits in which hydrocarbons are concentrated, occupying the small volume of reserves between the rock grains. Since the rock is permeable, this type of deposit is therefore easy to develop.

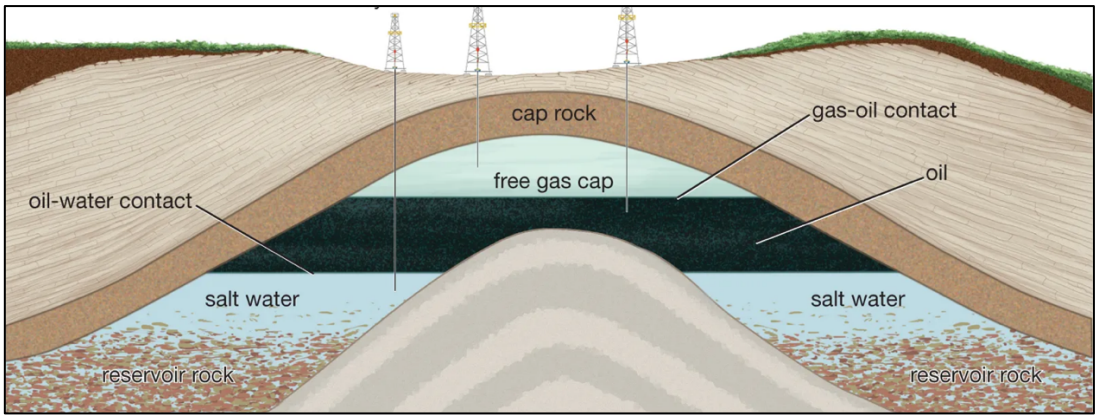

Figure 1: Conventional reservoir (Encyclopaedia Britannica, Inc 2012)

I.1.2 Unconventional reservoirs

Unlike conventional reservoirs, which have permeabilities greater than one-tenth of a milli-darcy, unconventional reservoirs have much lower permeabilities, measured in micro or even nano-darcies. In other cases (such as oil sands, heavy or extra-heavy oil), it is the quality of the oil that does not allow for conventional exploitation. The fluids contained in unconventional sources exist in large quantities but do not flow easily towards existing wells for economical recovery.

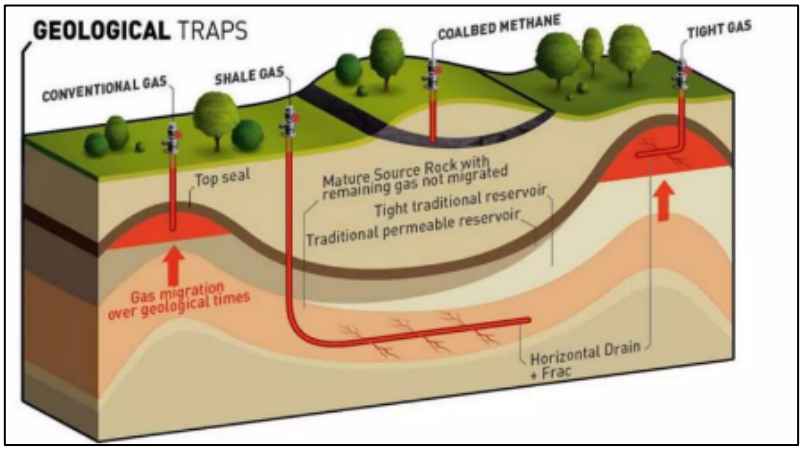

Figure 2: Unconventional reservoir (Oil and Gas Institute of Monastir)

I.2- Petrophysical characteristics of tight reservoirs

Tight reservoirs exhibit the following characteristics:

- Extremely low permeability, usually less than 0.1 millidarcy, typically found in sandstones that have undergone diverse stress conditions.
- Limited intergranular porosity.
- Severe fluid circulation constraints, rendering conventional techniques ineffective and necessitating increased effort for extraction.

I.3- Difficulties related to tight reservoirs.

Identify, evaluate, produce: these three classic steps for the oil industry transform into three challenges when dealing with tight reservoirs.

- **Identification:**

Identifying them is extremely difficult because the variation in acoustic characteristics, linked to the petrographic nature of the rock, is minimal. Moreover, the compact reservoirs are sometimes found at significant depths.

- **Evaluate:**

These geophysical studies are accompanied by significant petrophysical work. In order to measure the parameters of porosity and permeability of the formation, rock cores are extracted. It is then necessary to subject the samples to stress, meaning to place the rock back under reservoir conditions. This step is particularly critical: a small error in the stresses leads to significant differences in measurements, skewing these crucial parameters for exploitation. This delicate phase is complemented by information from well loggings, allowing for the accumulation of valuable data on the current stress directions to which the rocks are subjected. Better understanding of these data enables better design of hydraulic fracturing operations and maximization of reserves produced per well.

- **Produce:**

The naturally low productivity of wells, typical of so-called tight reservoirs, is generally insufficient to reach the economic threshold. The challenge is therefore to connect the maximum volume of rock to the well at an appropriate cost and thus reduce the number of wells to be drilled to produce the associated reserves. The identification and evaluation of reservoirs allow for the best determination of the type of well to be drilled: Vertical wells with hydraulic fracturing, Horizontal or highly deviated wells, Multilateral wells, or multi-fractured horizontal wells.

I.4- Techniques for exploiting tight reservoirs

Among the production techniques for tight reservoirs:

I.4.1. Hydraulic Fracturing

This process directly impacts the production of fluids present in compact reservoirs. It has been used in the oil industry since the early 1950s and aims to increase the productivity of oil, gas, and aquifer zones.

It aims to increase or restore the speed at which hydrocarbons can be produced and extracted from an underground reservoir, increasingly targeting unconventional reservoirs such as coal beds, shale formations, and compact (tight) reservoirs that could not be exploited by conventional methods. Hydraulic fracturing most often aims to enable the extraction of natural gas and oil from deep geological formations (often 1 to 4 kilometers, sometimes up to 5 kilometers). At these depths, the substrate is usually insufficiently porous or permeable to allow natural gas and/or oil to flow through the substrate to the well at a rate that makes the cost of the well profitable through the sale of hydrocarbons. Fracturing a targeted layer of rock containing hydrocarbons provides a conductive path connecting a larger area of the reservoir to the well, increasing the area surveyed by the well/fissure network system, from which natural gas and liquids can be recovered from the targeted formation.

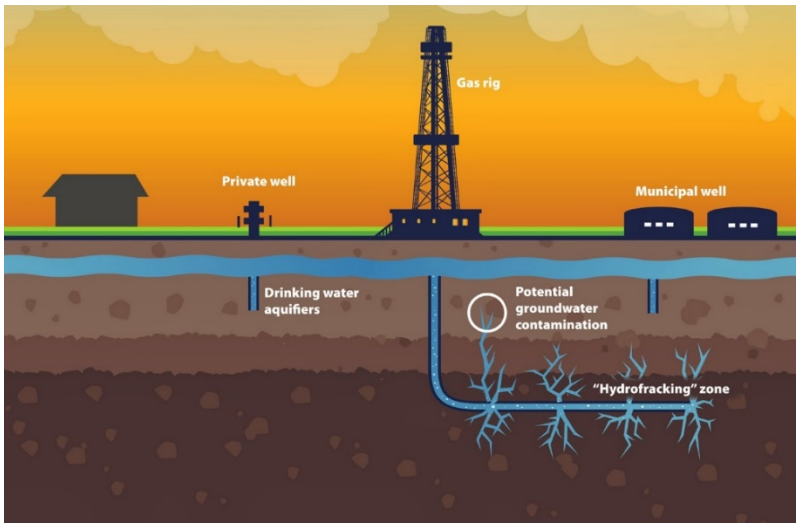

Figure 3: Hydraulic fracturing in an oil well

I.4.2. Short Radius (SR)

Short Radius is a new technique for well re-entry, primarily applied to dry, blocked, abandoned, or low-producing wells. It involves horizontally traversing intervals still containing hydrocarbons while avoiding zones with poor petrophysical characteristics. Well re-entry using Short Radius (SR for brevity), also known as "Re-Entry," was first applied in Algeria in the HMD field in 1995 in well MD 218. It is primarily adopted for dry or low-producing wells.

In this technique, horizontal drains are drilled from an existing vertical well, either cased or uncased. It involves horizontally traversing intervals still containing hydrocarbons (Yahiaoui, 2010).

Wells taken in SR have a curvature radius of less than 50m, sometimes even reaching 5m, and require specific equipment such as motors and articulated casings. Due to the difficulty of controlling the trajectory, the drain length is limited to approximately 300m, and such wells are challenging to complete, which limits the use of this technique (Belaid, 2005). Wells converted to Short Radius must meet the following conditions:

- Be a dry well or poor producer.
- Be far from injector wells to avoid aquifers and/or gas.
- Be in a low Gas-Oil Ratio (GOR) zone.
- Be in a non-tectonic zone to avoid faulted layers.
- The water table should be as low as possible.

The choice of the drain to be traversed by the Short Radius is generally based on the analysis of petrophysical characteristics:

- Porosity.
- Permeability.
- Water saturation.

To choose the drain, it is necessary to determine the most porous and permeable interval, also taking into consideration the water table.

The figure below shows the main components of the architecture of a Short Radius well, where:

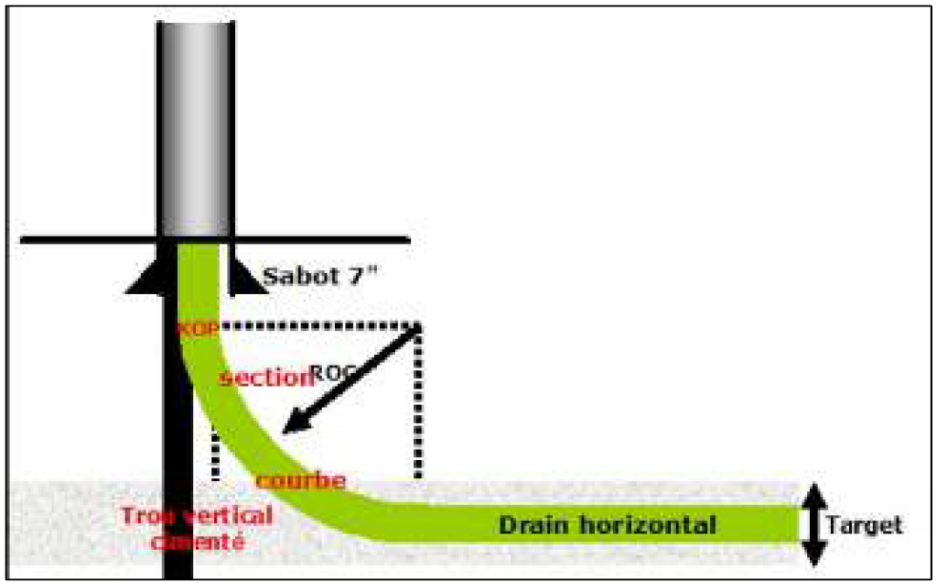

Figure 4: Architecture of a Short Radius well.

• KOP: Kick-Off Point, generally taken 10 meters below the casing shoe.

• Curve Section: This is the inclined part of the well (Length 60 to 70 meters and inclination 0 to 90 degrees).

• ROC: Radius of Curvature (± 40 meters).

• BUR: Build-Up Rate (7 to 15 degrees / 10 meters).

• Horizontal Drain (Length 300 to 500 meters): This is the well's objective, drilled horizontally inside the target drain with a specified tolerance in vertical depth called the drain.

II. Pressure.

II.1- Pressure Concepts

Prior to initiating drilling operations in any global location, it is imperative for the driller to possess knowledge and comprehension of the diverse pressures existing within the subsurface, which will interact with the ground during drilling activities. The distinct formation pressures experienced within a region significantly influence both the exploration and exploitation phases of potential hydrocarbon reserves.

II.2- Types of pressure

The various types of reservoir pressure commonly encountered during the drilling phase are generally divided into three main components:

- Hydrostatic Pressure.
- Overburden Pressure (Vertical).
- Formation Pressure.

II.2.1- Hydrostatic Pressure

It is defined as the pressure exerted by a column of fluid extending from a layer to a surface. Hydrostatic pressure is caused by the unit weight and vertical height of a fluid column. The size and shape of this fluid column have no effect on the magnitude of this pressure: It is expressed by the general formula: $\{ PH=\rho.g.h \}$

Where:

PH: hydrostatic pressure.

ρ: average density.

g: gravity value.

h: height of the column.

This pressure can be expressed differently with the relationship below:

Hydrostatic pressure = pressure gradient ∗ true vertical depth[1]

The hydrostatic pressure gradient is affected by the concentration of dissolved solids and gases in the fluid column at different or varying temperature gradients. An increase in dissolved solids slightly increases the normal pressure gradient, while an increase in the amount of gas in solution at a higher temperature would decrease this gradient.[2]

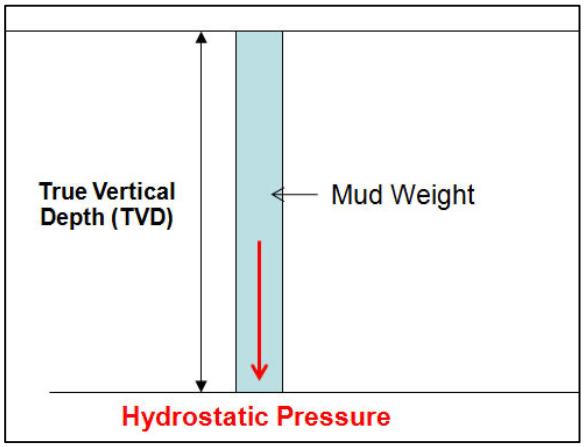

Figure 5: Hydrostatic Pressure in a Column

II.2.2- Overburden Pressure (Vertical Stress)

The total vertical pressure (stress) at a given depth is referred to as overburden pressure. In other words, it is the weight of the overlying formation, which includes the matrix pressure (grain-to-grain compaction) and the pressure of fluids within the pores

[1] M. B. a. A. Hamid, "Pore Pressure Prediction in Shale Gas Field,", March.
[2] A. R. Ismail, drilling engineering, Malaysia, 2011.

(formation pores)[3]. The term "Overburden" is often attributed to this vertical stress. Determining the Overburden Gradient (OBG) helps estimate the pressure at which the rock will break or fracture, known as the fracturing pressure.

The figure below illustrates the concept of vertical stress (overburden) with a graphical representation:

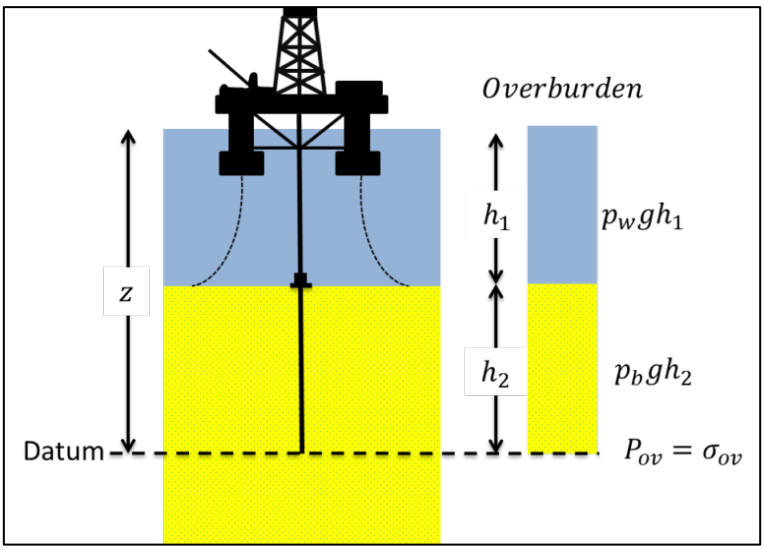

Figure 6: Factors of Overburden Pressure (Vertical)[4]

One can say that the stress or overburden pressure (OBP) at a certain depth (datum) is equal to the total sum of all pressures above this reference point. These pressures result from the weight of the fluid column and the pressure of the water column. It is also important to note that pressure can be calculated at the exact point using the bulk density ρ*b*, rather than the density of grains or fluids.

The pressure gradient OBG, which relates OBP pressure to depth, is often discussed. This term is commonly used in such pressure studies.

It can be stated that at any point on the Earth's surface, the overburden pressure (OBP) is the sum of stresses from the rock mass and the fluid above a certain point of interest. It is important to note that the density used in calculating overburden pressure is the bulk density, which considers both the density of rocks and the present fluids.

II.2.3 Pore pressure

Pore pressure (interstitial) is defined as the pressure acting on fluids in the interstitial spaces of the rock. This pressure is generally referred to as formation pressure (pore pressure). Depending on its magnitude, it can be described as normal, abnormal, or subnormal.

[3] G. M. a. A. N. J. Dvorkin, “Overpressure detection from compressional- and shear-wave data,” Geophys. Res. Lett., vol. 26, no. 22, pp. 3417–3420,, 1999.
[4] Overburden Pressure: What is it and Why is it important? – Top Dog Engineer.”," [Online].

II.2.3.1 Normal pore pressure

Normal pore pressure is equal to the hydrostatic pressure of a formation fluid column extending from the surface to the subsurface.

In other words, if the formation were open and filled with a column whose length equals the depth of the formation, then the pressure at the bottom of the column would be equal to the formation pressure, and the pressure at the surface would be zero.

Normal pore pressure is not constant. Its magnitude varies depending on the concentration of dissolved salts, the type of fluid, the presence of gases, and the temperature gradient.

For example, when the concentration of dissolved salts increases, the magnitude of normal pore pressure increases. (Rabia, 2002)

II.2.3.2 Subnormal pore pressure

Subnormal pore pressure refers to any formation pressure that falls below the hydrostatic pressure of the corresponding fluid at a given depth.

These pressures are less prevalent compared to abnormal pore pressures and often manifest long after the formation's deposition. Subnormal pressures may arise from natural factors associated with the stratigraphic, tectonic, and geochemical history of an area, or they may be artificially induced by the production of reservoir fluids[5].

II.2.3.3 Abnormal pore pressure

Abnormal pore pressure is defined as any pore pressure that exceeds the hydrostatic pressure of the formation water occupying the interstitial space. It consists of a normal hydrostatic component and an additional pressure. Abnormal pore pressure can occur at various depths, ranging from a few hundred feet to over 25 meters deep, and may be due to a combination of geological, geochemical, geothermal, and mechanical factors. Possible origins of abnormal pressure generation include fluid pressure level, reservoir rock compaction, faults, salt diapirism, and diagenetic phenomena [6] [7].

[5] H. (Rabia, Well Engineering & Construction, London, 2002.
[6] H. (Rabia, Well Engineering & Construction, London, 2002.
[7] N. Adams, Drilling Engineering, Tulsa, Oklahoma: Penn well publishing company, 1985.

Pressure Relationships

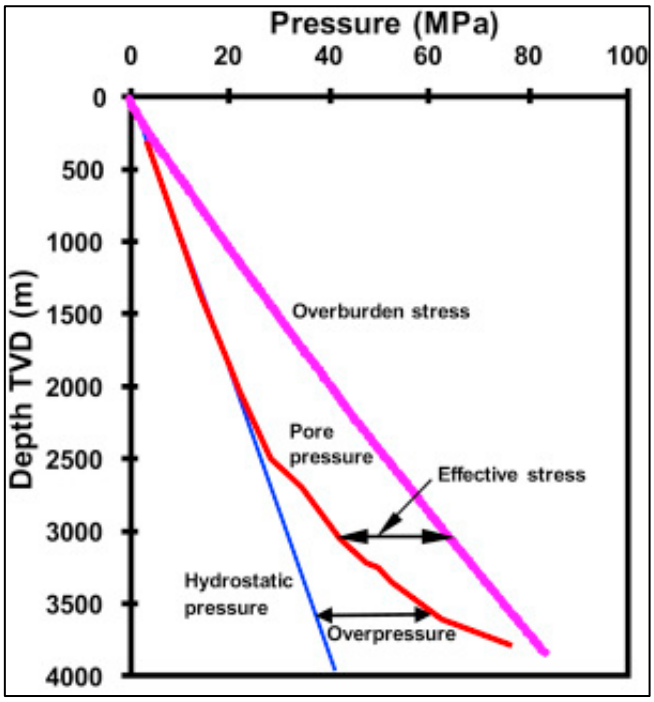

Figure 7: Pressure Relationship as a Function of Depth

Pressures can be differentiated from normal pressure as follows[8]:

I. If Pp > Phyd: abnormal pressure (overpressure).
II. If Pp < Phyd < Pf: normal pressure.
III. If Pp < Phyd: subnormal pressure (underpressure).

Overpressures are more common than underpressures.

II.2.3.3.1 Drilling problems related to abnormal pressure

Abnormal pressures affect the drilling plan in many areas, including the following:

- Casing design.
- Selection of mud weight and type.
- Selection of casing setting depth.
- Cement planning.

Additionally, the following issues must be considered due to high pressures in formations:

- Kicks and blowouts.
- Differential pressure rod sticking.
- Loss of circulation due to high mud weights.
- Well costs increase significantly with Geo pressure.

[8] B. G. Z. H. W. D. H. N. a. T. J. Z. Liu, "“Pore characteristics and formation mechanism of high-maturity organic-rich shale in Lower Cambrian Jiumenchong Formation, southern Guizhou,”," Vols. vol. 3, no., no. 10.1016/j.ptlrs.2018.03.002., p. mars, 2018.

Due to the challenges associated with high-pressure exploration well planning, most design criteria, publications, and feasibility studies are not considered.

Most design criteria, publications, and studies have been dedicated to this field; the efforts made are justified[9].

III. Fracturing.

III.1- Hydraulic fracturing.

commonly known as fracking, is a process that directly impacts the production of fluids present in compact reservoirs. It has been used in the oil industry since the early 1950s with the aim of increasing the productivity of oil, gas, and aquifer zones.

Stimulation artificially enhances the permeability of the rock. While conventional and unconventional reservoirs may suffice with chemical treatments such as acidification, these methods are insufficient for extracting hydrocarbons trapped in shale rock or in compact reservoirs with low petrophysical parameters. Consequently, the industry often resorts to fracturing processes, also known as stimulation, with hydraulic fracturing being a specific mechanical category.

The objective of fracturing is to create microfractures or reactivate the natural fracture network within the rock to facilitate hydrocarbon flow. While it is now used for other purposes like geothermal energy, its effectiveness in the oil and gas sector has been proven (OECD, 2014). Essentially, it involves reopening or artificially creating a network of small fissures around a well, enabling the drainage of hydrocarbons located a few meters away. The extent of this drainage zone varies depending on the environment and the technique used.

Hydraulic fracturing is currently the predominant technique used for exploiting unconventional reservoirs. However, the properties of the reservoir and surface environmental characteristics may lead to the selection of alternative technologies.

[9] N. Adams, Drilling Engineering, Tulsa, Oklahoma: Penn well publishing company, 1985.

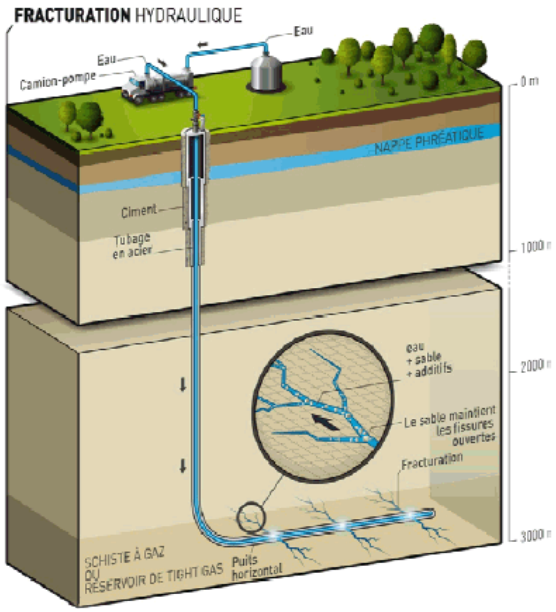

Figure 8: Conceptual diagram of hydraulic fracturing (Total)

- **History of hydraulic fracturing:**

Hydraulic fracturing is not a recent invention; it was first performed in the United States in 1947 and later in the USSR around 1954. It has been developed for 70 years, preceding the implementation of the first horizontal drilling. It is a technique considered mature by industry, with 1.2 to 2 million fracturings performed in the United States alone, accounting for 50,000 wells per year in 2013 (Lenoir et al., 2013).

In Algeria, particularly, hydraulic fracturing is a relatively old stimulation technique. It was first introduced in 1960 in well OM6 of the Hassi Messaoud field. However, it wasn't until the early 1990s that it was regularly applied in the same field (In Atlili, 2016). This transition occurred due to several reasons deduced after analyzing 25 hydraulic fracturings, including the lack of understanding of the state of minor geostatic stress prevailing in the Cambrian.

III.2- Constraints related to fracturing.

Fracturing moves in the direction of least resistance, meaning the fracture propagates perpendicular to the minimum stress.

The figure below shows that beyond a certain depth, the magnitude of the horizontal stress becomes weaker than the vertical stress. The principal stresses are noted as $\sigma_V > \sigma_H > \sigma_h$ in the typical case. σ_V represents the vertical principal stress, or geostatic stress, also known as the weight of the overlying rock.

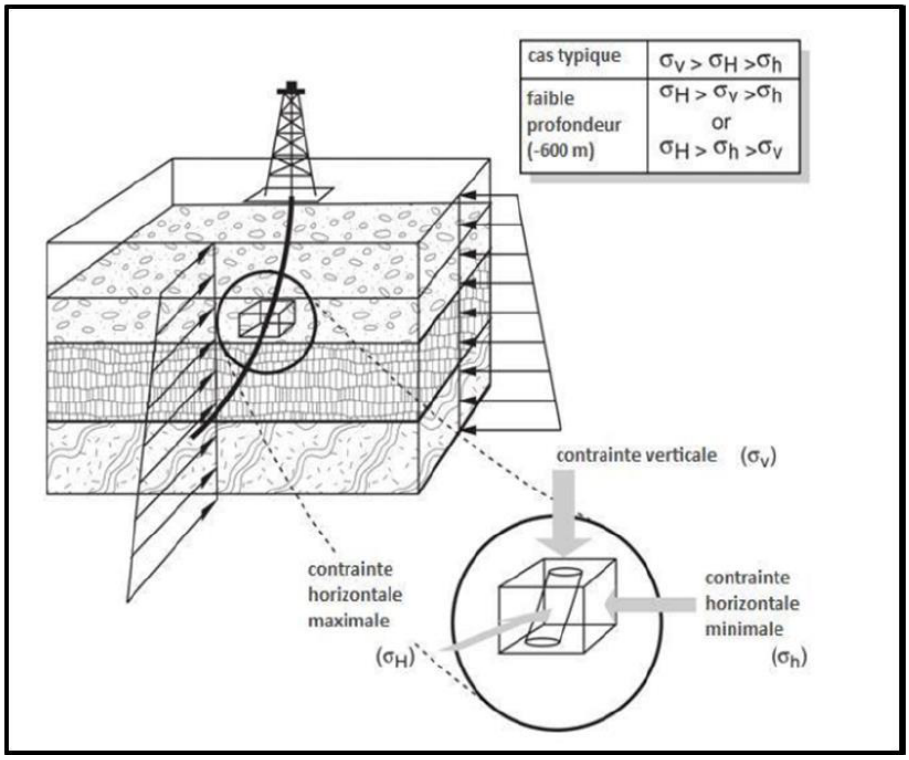

Figure 9: Schematic representation of stresses

III.3 Selection of zones for fracturing in Tight reservoirs

The success or failure of a hydraulic fracturing treatment often depends on the quality of the candidate well chosen for this treatment. Selecting an excellent candidate for fracturing often ensures success, while choosing a poor candidate typically results in economic failure. To select the best candidate, many variables must be considered. The most critical parameters for hydraulic fracturing include formation permeability, in-situ stress distribution, reservoir fluid viscosity, Skin effect, reservoir pressure, reservoir depth, and bottom hole condition. The Skin effect refers to whether the reservoir is already stimulated or possibly damaged. Generally, if it is positive, the reservoir is damaged and will likely be an excellent candidate.

The best wells for hydraulic fracturing treatments in compact reservoirs have a substantial volume of OOIP (Original Oil In Place) and good barriers for vertical fracture growth above and below the net pay intervals. Such reservoirs have:

- A thick net pay (productive zone).
- Medium to high pressure.
- In-situ stress barriers to minimize vertical fracture height growth.
- Considerable reservoir surface area.

Additionally, reservoirs lacking sufficient clean clays above or below the net pay, which suppress vertical fracture development, are considered poor candidates. Those with extremely low permeability may not produce enough hydrocarbons to cover all drilling

and completion costs, even if successfully artificially fractured; thus, such reservoirs would not be good candidates for stimulation (SPE, 2018).

III.4 Contribution of Geomechanics in Hydraulic Fracturing

The origins of geomechanics in the oil industry were rooted in hydraulic fracturing, where simulation engineers sought to understand the pressures required from the drilling well to overcome the formation and fracture the rock, as well as estimate the probable extent and direction of induced fractures.

Later on, geomechanics began to be applied to predict and avoid drilling and production issues such as sand production, wellbore instability, unsuccessful hydraulic fracturing, etc.

The first step of every geomechanics-related process is to construct a 1D geomechanical model or 1D Mechanical Earth Model (1D MEM). Essentially, the 1D MEM is a numerical representation of the mechanical properties of rocks as well as the stress state for a specific lithology or stratigraphic section in a well (Plumb, Edwards, Pidcock, Lee, & Stacey, 2000). This can help overcome geomechanical issues resulting from overpressures, wellbore instability, hydraulic fracturing breakdown, sand production, reservoir compaction, and casing failure.

Until about a decade ago, rock mechanical properties and stress conditions were often overlooked, and particular attention was not paid to geomechanical issues. An accurate MEM can significantly save time and drilling costs by preventing and/or avoiding certain problems that occur during drilling or production.

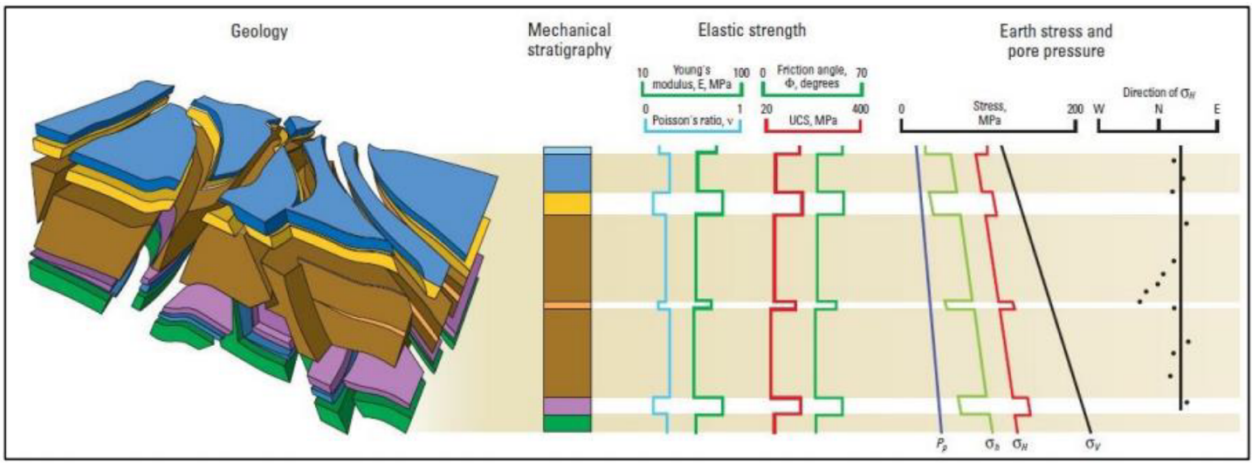

Figure 10: The concept of the 1D geomechanical model (1D MEM)

Geomechanics plays a very important role in a hydraulic fracturing program. Indeed, through a stress profile obtained by combining various elastic and mechanical parameters of the targeted formation, one can determine the zones of minimum stress which represent the areas of interest to be fractured. Additionally, one can calculate the deformation and massive rupture caused by hydraulic fracturing and determine the final geometry of the fracture.

Chapter II: Presentation of the Study Area

I. Presentation of Hassi Tarfa Field (HTF)

I.1 Geographic location

The Hassi TARFA field lies on the outskirts of Hassi Messaoud, constituting a satellite structure extending southward into Block No. 427. It occupies the transitional area between the Hassi-Dzabat permit and the Hassi Messaoud field. Its boundaries are defined by the 31° and 32° North parallels, and the 6° and 7° East meridians.

Situated within the Triassic province, south of the Hassi Messaoud deposit, along the El Gassi-El Agreb-Hassi Messaoud trend border, the Hassi TARFA structure is depicted in Figure 11.

The Hassi TARFA field is surrounded by various features:

- To the North and Northeast lies the Hassi Messaoud field.
- To the West is the anticlinal structure of Hassi D'zabat.
- The Mesdar field lies to the East.
- To the South is the El Gassi field.

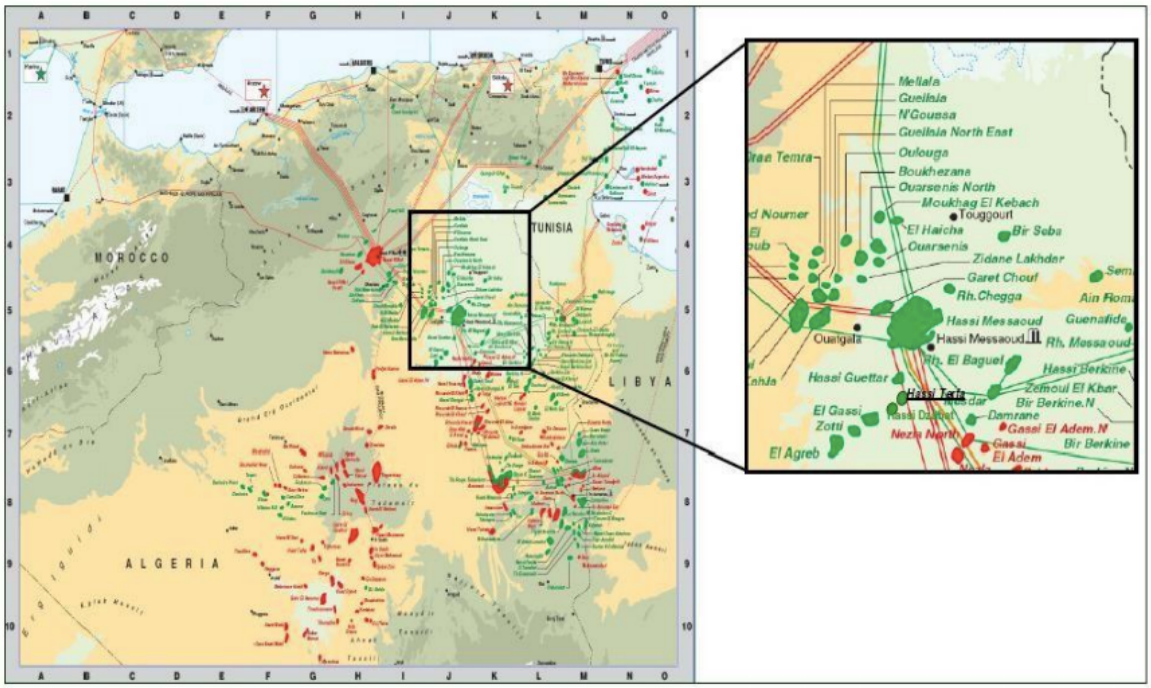

Figure 11: Location of the Hassi Terfa Field (DP-SONATRACH)

I.2 Field history

The Oued Mya basin stands as one of Algeria's most prolific regions, boasting rich reserves in areas like Haoud Berkaoui, Berkaoui – Benkahla, Guellala, Kef El Agroub, Drâa Et Tamra, and Boukhezane. Among these reservoirs, Hassi Tarfa (HTF) emerged as a recent discovery, signifying a promising addition to the region's hydrocarbon landscape. The exploration journey began with the drilling of HTF-1 in September 1999,

strategically positioned amidst established oil-producing fields like Hassi Messaoud, El Agreb Zotti, and El Gassi within the Cambrian strata.

Initially, HTF-1 aimed at evaluating the Cambrian reservoirs Ri and Ra, with a secondary interest in the Quartzites de Hamra. While the Ri and Ra formations proved to be aquifers, the Quartzites de Hamra revealed oil-bearing potential, hinting at the reservoir's significance in future endeavors. This initial success spurred further exploration, leading to the drilling of subsequent wells, HTF-2, HTF-3, and HTF-4, over the following years.

In 2001, HTF-2 and HTF-3 were drilled, primarily focusing on delineating the structure and evaluating the productivity of the Quartzites de Hamra. HTF-3, in particular, played a pivotal role in not only assessing the reservoir's potential but also testing its viability within the structural confines and delineating the extent of the Ordovician reservoir within the structure. These efforts aimed not only to confirm reserves but also to understand the geological complexities of the Hassi Tarfa field.

By May 2005, the exploration efforts culminated in the drilling of HTF-4, which furthered the evaluation of the Quartzites de Hamra and the Cambrian sandstones of the Ri and Ra levels. The collective data obtained from these drilling campaigns provided crucial insights into the reservoir characteristics, structural integrity, and hydrocarbon potential of the Hassi Tarfa field.

Illustrating the evolution of drilling activities over two decades, the progression from HTF-1 to HTF-4 highlights the systematic approach taken to unlock the hydrocarbon potential of the Hassi Tarfa structure within the dynamic landscape of the Oued Mya basin. This journey underscores the meticulous exploration efforts aimed at delineating reservoirs, confirming reserves, and maximizing the field's production potential for the benefit of Algeria's energy sector.

I.3 Lithostratigraphic Overview

The stratigraphic sequence of the Hassi Tarfa region is primarily composed of Mesozoic deposits, spanning 3118 meters in thickness. These deposits rest unconformably on the Palaeozoic, which measures 407 meters in thickness. Finally, a thin spread of tertiary-age detritus, approximately 300 meters thick, lies discontinuously over the Mesozoic.

1- Paleozoic:

The detrital sequence identified by drilling is composed of Cambro-Ordovician formations. These formations are dominated by large regional spreads of coarse detrital rocks that prograded from south to north unconformably over a heterogeneous basement affected by the Pan-African phase. These formations are overlain by thick series of clay and sandstone resulting from major marine transgression-regression periods originating

from the north. The Cambro-Ordovician occasionally experiences volcanic episodes with limited lateral extent. During the Silurian period, a major global transgression from the north was characterized by organic black clays with graptolites in a highly un-oxygenated environment.

2- Mesozoic:

The clayey-sandstone detrital rocks dated from the Upper Triassic mark the beginning of the Mesozoic sedimentary sequence with an angular unconformity over the Paleozoic strata. Across the northern region, these deposits correspond to a period of slow marine regression originating from the East.

Throughout this territory, a continental influence is evident, marked by the establishment of a... After a phase of rifting, accompanied by volcanic eruptions at the base of the Triassic, follows a period of evaporitic deposits lasting from the late Triassic to the early Jurassic.

The evaporitic deposits are represented by dolomitic intervals, oolitic limestone, or marl-carbonate layers.

The Lower Cretaceous is characterized by extensive sandstone deposits, a result of regression interrupted by a transgressive Aptian carbonate interlude.

The Cenomanian-Turonian is marked by a resumption of the transgressive cycle. It begins with a phase of lagoon-influenced sedimentation evolving laterally and vertically into marine facies.

3- Cenozoic:

During the Tertiary period, deposits characteristic of epicontinental and lagoon platforms persisted throughout the Paleocene and Eocene; this period is marked by the Alpine orogeny and its compressive phases.

Lithological Description

The lithological description depicted in the following column (Figure No. 02) was conducted using technical data sheets from various wells in the Hassi Tarfa field.

Stratigraphic commentary

1- Paleozoic:

➢ Cambrian: It is represented by three levels, Ra, Ri, and the alternating zone.

✓ Ra: It is characterized by its heterogeneous facies with horizontally stratified and rarely distinctly cross-bedded layers visible in the cores. This continental-origin succession is characteristic of fluvial sequences, with a constant thickening gradient.

✓ Ri: Its facies are homogeneous with sub-horizontal stratification, belonging to a shallow coastal marine environment. The thickness is almost constant at HTF-1 (49m).

✓ Alternating Zone: This isopaque formation exhibits oblique, sometimes horizontal stratifications, and levels with numerous tigillites. It is characteristic of a marine environment with continental influence, and this zone shows no lateral facies changes in the region. The thickness is (29m) at HTF-1, (13m) at HTF-2 and HTF-3.

➢ Ordovician: It is eroded by the Hercynian phase down to the level of Ouargla Sandstones; the Ordovician is represented by four terms.

✓ El-Gassi Clays: This homogeneous unit, with its argillaceous-silty thickness, indicates sedimentation in a transgressive marine environment.

✓ El-Atchane Sandstones: They exhibit oblique to sub-horizontal stratifications and numerous clay pebbles, indicating a coastal marine environment.

✓ Hamra Quartzites: They are notable on the surface for their massive morphology and poorly preserved sedimentary structures. Intense fissuring is typical of this layer, originating from a coastal environment with rare marine fluctuations. The Hamra Quartzites show no facies variations in the region. They have relatively the same thickness: HTF-1 (116m), HTF-2 (104m), HTF-3 (126m).

2- Mesozoic:

➢ Triassic: It is poorly developed in the region or eroded by the Hercynian phase, represented only by igneous rocks and the Lower Series. Its environment is a meandering fluvial setting. The thickness is much greater towards HTF2 to the west (68m).

➢ Jurassic: The differentiation of an evaporitic environment initiated during the clayey Lias continues through the Jurassic. Substantial subsidence during the Lias period shows thick salt series accompanied by sporadic openings to the sea. The Jurassic thickness has a gradient from south to north; HTF-2 (1333m), HTF-1 (1361m), HTF-3 (1372m).

➢ Cretaceous: The lower member, characterized by continental detrital sedimentation, is the result of a regression towards the north, interspersed with a transgressive marine episode during the Aptian. The upper member, predominantly carbonate in facies, is intercalated with evaporitic deposits.

3- Cenozoic:

During the Tertiary, sedimentation of an epicontinental and lagoon platform type continues during the Eocene, which unconformably overlies the carbonate Senonian.

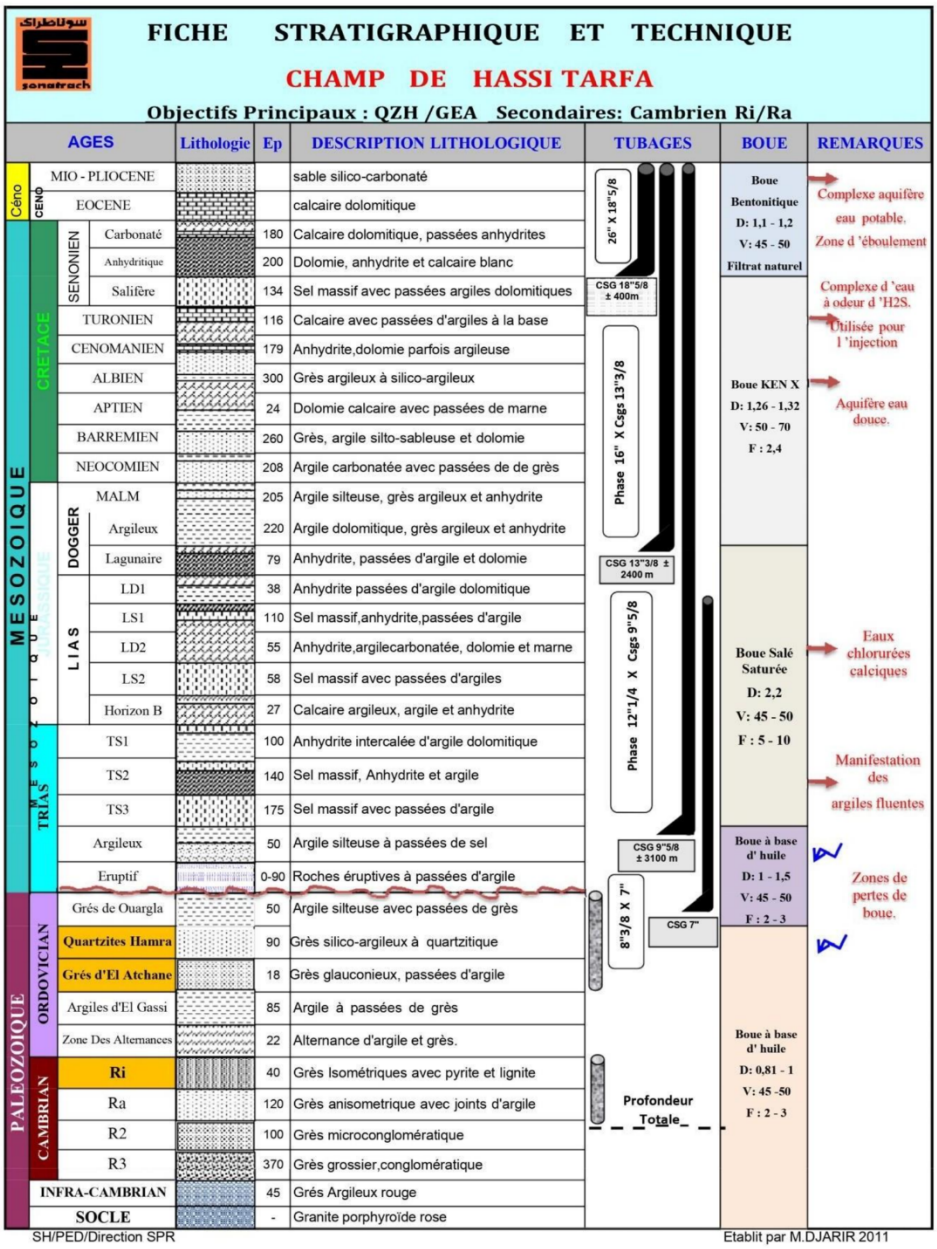

Figure 12: Stratigraphic Column of the Hassi Tarfa Region (Sonatrach-DP HMD 2011)

II.4 Structural aspect

Tectonic Evolution and Known Phases

Ante-Paleozoic Deformations:

- **Pan-African Phase:**

It is interpreted as the result of continental collision between two cratons:

▪ The rigid West African craton.

▪ The more plastic East African craton.

This stress regime persisted until the Cambrian and resulted in a network of faults-oriented North-South and Northeast-Southwest, which later played a significant role in structuring the Saharan platform. The Tuareg Shield initiated during this period.

Paleozoic Deformations:

- **Taconic Phase:**

This phase corresponds to a compressive movement oriented west, resulting in regional uplift. The Reguibat and Tuareg Shields underwent erosion. Simultaneously, significant climate change triggered the formation of an ice cap in central Sahara. Its melting led to a widespread transgression across the Sahara. A period of extension follows this compressive phase during the Silurian.

- **Lower Devonian Phase:**

Thickness variations along faults, as well as volcanic flows, indicate a period of extension during the Siegenian-Gedinnian.

- **Hercynian Phase:**

This is the main phase that generated trends oriented northeast-southwest in the Oued Mya depression.

- **Middle and Upper Devonian:**

A compressive movement caused the gradual uplift of the Hassi Messaoud area, shifting the center of the Oued Mya depression westward, where Devonian deposits developed east of the Allal arch.

- **During the Middle Carboniferous and Late Permian:**

Another compressive movement occurred, accelerating the uplift of the Oued Mya basin, which became a high emerged plateau. This prevented Carboniferous deposition in this area. At the end of the Hercynian orogeny, erosion of the relief was intense, sometimes reaching the basement; however, in the study area, the youngest Paleozoic formation is the Silurian.

Mesozoic Deformations:

- **Triassic Rifting Phase:**

In the Upper Triassic, there is an onset of rifting accompanied by extensive volcanic rock eruptions. Subsidence was significant during the Hettangian. A rift oriented Northeast-Southwest begins to take shape, bordered by faults of the same direction.

- **Austroalpine Phase:**

It is characterized by an East-West shortening phase leading to significant structuring along sub-meridian faults. North-South axis anticlines allowed for hydrocarbon accumulation. This phase is the origin of tectonic inversion. At the Albian stage, a relaxation phase occurred; it persisted at least until the Turonian accompanied by a marine transgression.

- **Pyrenean Phase:**

At the end of the Eocene, there is an uplift of structural zones, creating Northeast-Southwest axis anticlines, which were well expressed at the end of the Miocene.

- **Atlasian Phase:**

In the Villafranchian, a North-South directed shortening affects the northern part of the Oued Mya basin, resulting in uplift of its southern part.

Local Framework:

The structure of Hassi Tarfa belongs to the northern extension of the El Agreb-Hassi Messaoud axis, within which various anticlinal folds of NE-SW orientation are inserted, sometimes intersected by smaller sub-meridian faults.

The current structural image is the result of polyphased tectonics that have affected the region since the Pan-African orogeny; the Hercynian phase is the most significant along the El Agreb-Hassi Messaoud trend and its associated structures.

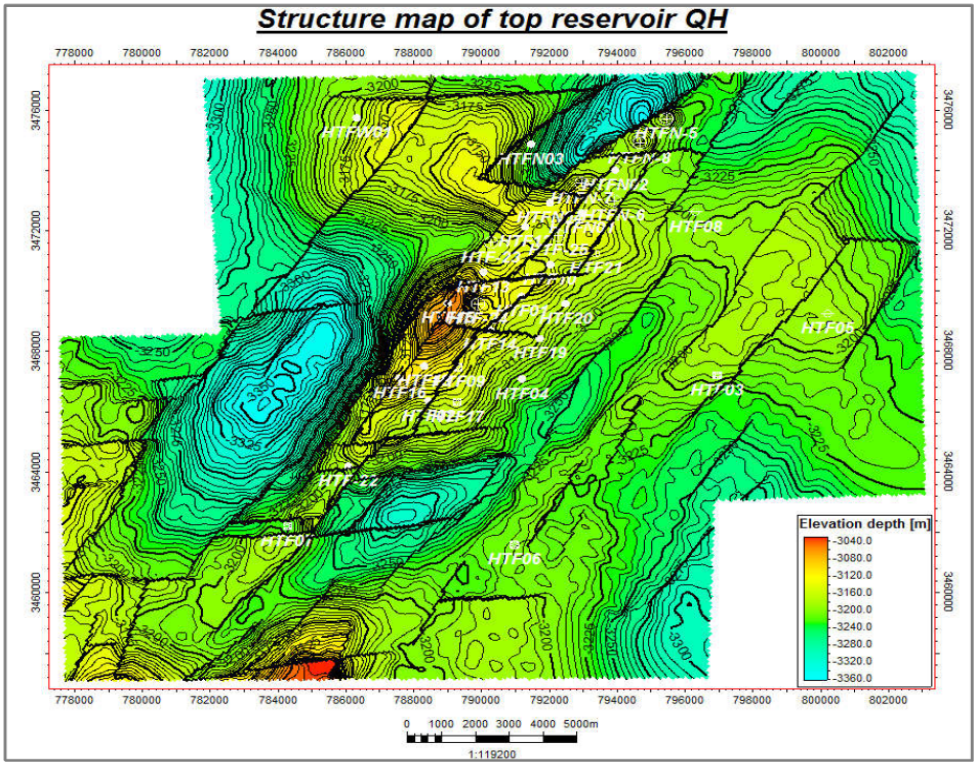

Figure 13: Structural map of Quartzite Hamra top in Hassi Tarfa field

The individualization of structures occurred during the Paleozoic. Tectonic movements during the Jurassic and even the Present have also had a significant impact on the final structural pattern, where locally, horsts and mini-grabens can be distinguished. The Hassi Tarfa field has an elongated anticlinal shape, oriented NE-SW, with closure against a fault to the west. It is bordered by major and minor faults of the same direction.

II.5. Petroleum system

In the realm of petroleum geology, the idea of a petroleum system has been defined by scholars like A. Perrodon and I.C. White as a geographical area meeting the geological prerequisites for the presence of oil and/or natural gas reservoirs.

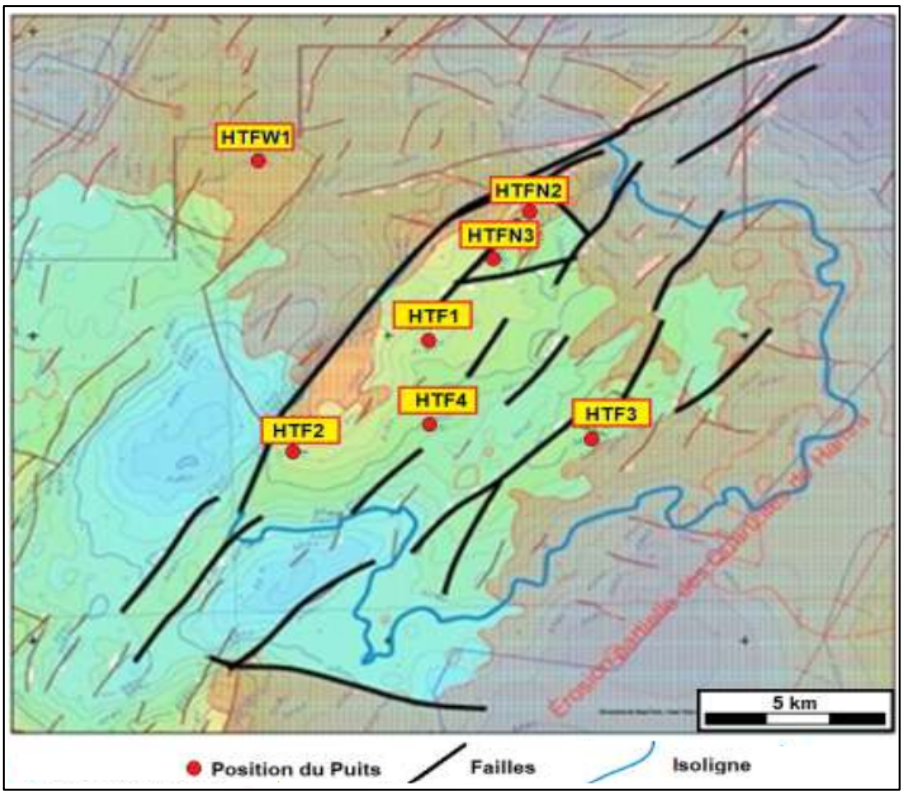

Figure 14: Isobath map at the top of the Hamra Quartzites

A set of conditions is required for a given area to contain reserves of oil and/or natural gas. These may include:

- Existence of a sufficiently organic-rich source rock,
- Presence of a porous layer above this source rock, capable of serving as a reservoir,
- Existence of an impermeable layer above the reservoir, preventing the oil from escaping,
- Presence of structures capable of trapping the oil: anticline, fault trap, deformation by a salt dome,
- Sufficient maturation of the source rock, allowing for the generation and expulsion of hydrocarbons.

When an oil company initiates exploration in a new region, its primary aim is to demonstrate the presence of all these elements, in other words, to confirm the existence of a functional petroleum system. Three provinces have been analyzed for evaluation in this regard. Firstly, the province of the Triassic/Ghadames Basin, located east of Algeria, south of Tunisia, and at the extreme west of Libya, generally coincides with the Triassic basin of the Mesozoic age. This basin partially or fully overlaps with the Melrhir Basin, the Ghadames or Berkine Basin, and the Oued Mya Basin, of Paleozoic age. Secondly, the Illizi Basin province is situated in eastern Algeria and the extreme west of Libya. Thirdly, the Grand Erg/Ahnet Basin province is primarily located in western Algeria but extends slightly into Morocco. The Grand Erg/Ahnet Basin province includes the Timimoun Basin, the Ahnet Basin, the Sbaa sub-basin, the Mouydir Basin, the Benoud Basin, the Bechar/Abadla Basin, and a part of the Oued Mya Basin. The composite total petroleum systems identified in the provinces of Triassic/Ghadames, Illizi, and Grand Erg/Ahnet are as follows: Tanezzuft-Oued Mya, Tanezzuft-Melrhir, Tanezzuft-Ghadames, Tanezzuft-Illizi, Tanezzuft-Timimoun, Tanezzuft-Ahnet, Tanezzuft-Sbaa, Tanezzuft-Mouydir, Tanezzuft-Benoud, Tanezzuft-Benba, and Tanezzuft Mouydir. "Tanezzuft" refers to the Silurian Tanezzuft Formation, which is the oldest major source rock of these total petroleum systems. The second name refers to the basins in which the total petroleum systems exist.

In the petroleum system, we typically have the mother rock, reservoir rock, and cap rock. However, in the case of HTF, we only have the reservoir rock and cap rock.

II.5.1 Reservoir rock

In the Ordovician, the most significant reservoir is formed by the Hamra Quartzites, with significant proven oil quantities around the Hassi Messaoud field.

II.5.2 Cap rock

The clay-salt formations of the Lias and the Triassic eruptive rocks serve as excellent cover rocks for the Hamra Quartzites.

Traps and Migration Pathways

The majority of traps in the Cambro-Ordovician reservoirs are related to:

- either structural traps (horsts, anticlines),
- or stratigraphic traps (erosion truncation bevels of Hercynian erosion),
- or mixed traps (Ordovician bevels upstream dip of an anticlinal structure). Geochemical studies define two periods of migration:
- The first occurs at the end of the Paleozoic.
- The second, which is more significant, occurs towards the end of the Jurassic and the beginning of the Cretaceous.

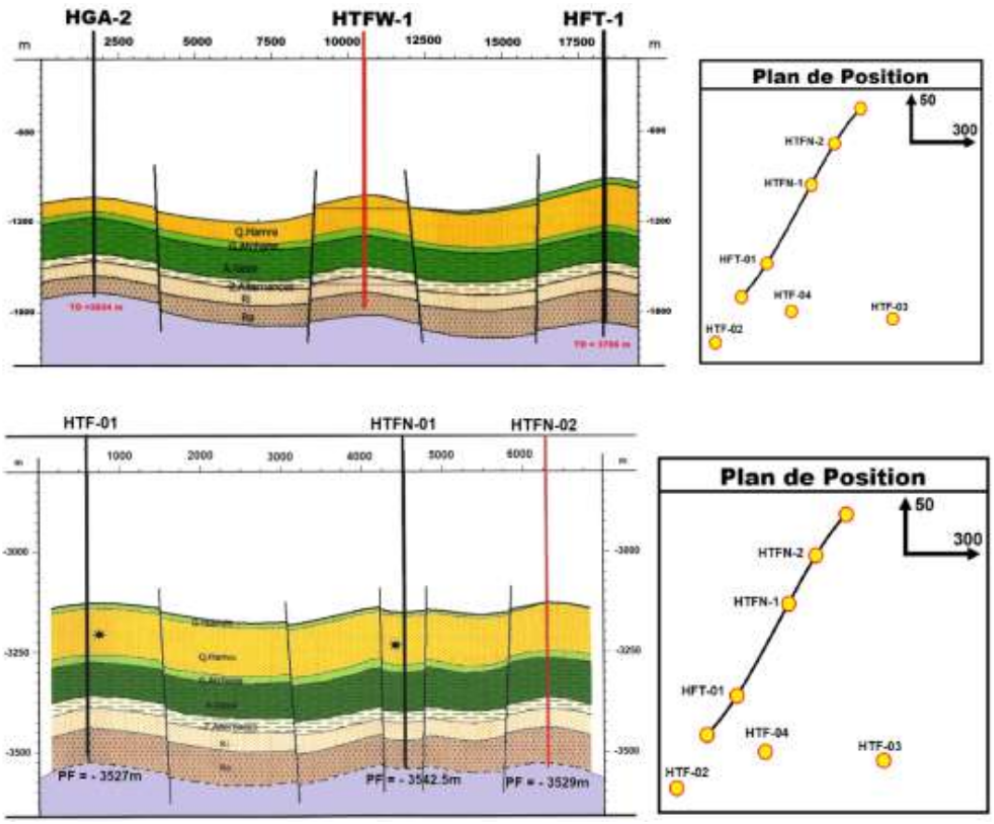

Figure 15: Geological cross-section NW-SE (Exploration Department, SONATRACH)

III. Case study Well HTF-19.

III.1 Geographical location

Well HTF-19 is located in the central part of the Hassi Terfa perimeter.

Geographical Coordinates. Longitude: 6° 03' 54.19280" E. Latitude: 31° 18' 58.89979" N

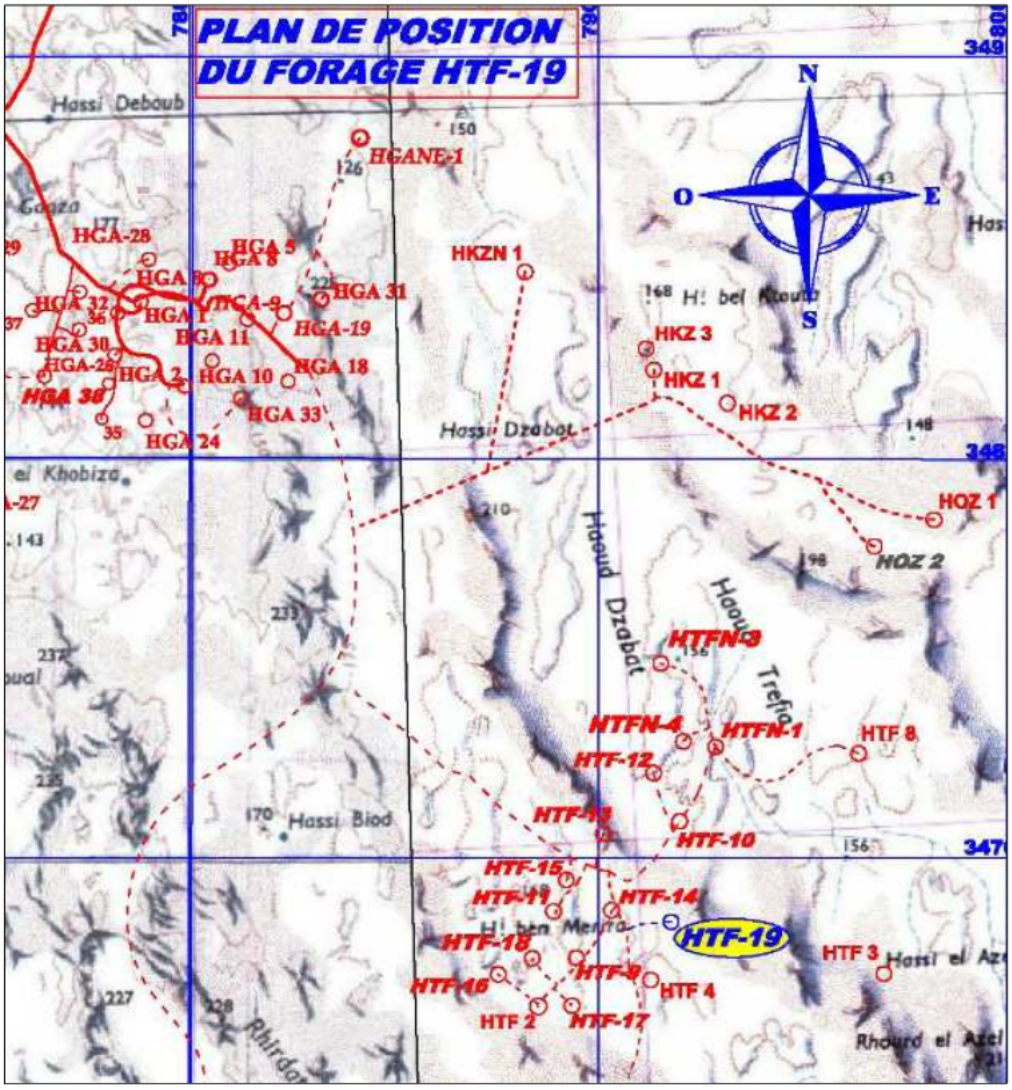

Figure 16: Positioning plan of Well HTF-19

III.2 The geological framework

The petroleum interest of this well primarily focuses on the Hamra Quartzites. This unit exhibits a relatively high structure-oriented NE-SW, which is capped by the Hercynian unconformity. The average thickness of the Hamra Quartzites in the Hassi Tarfa field is around 110 m . Hercynian erosion in the Hassi Tarfa field is very pronounced in the northwest part of the perimeter where the thickness of the Quartzites is low, ranging from 50 to 90m, while it is thicker towards the southeast (110-150m). Well HTF-19 is located east of the main, relatively low structure, where the thickness of the Hamra Quartzites is significant, estimated at 119m.

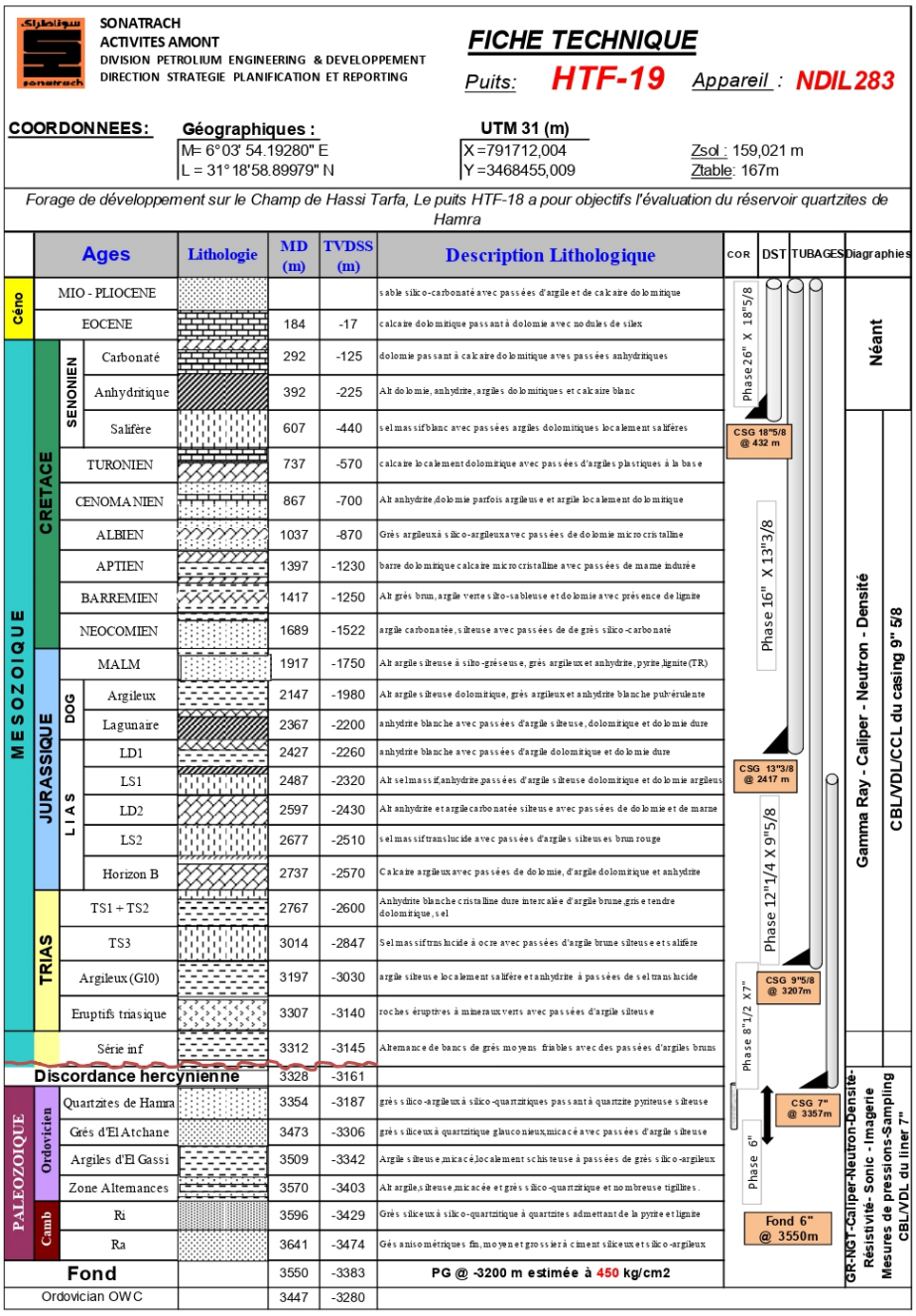

Figure 17: Technical data sheet of well HTF-19 (RDI HTF19 SH-DP-HMD)

III.3 Structural aspect

The Hassi Tarfa field exhibits a structure-oriented NE-SW, affected by some faults running NW-SE and a major fault running NE-SW that divides this field into two zones, a high zone to the east and a low zone to the west. The throw of this fault is approximately 50 m.

III.4 Petrophysical Characteristics

The petrophysical characteristics of the Hamra Quartzites in the Hassi Tarfa field are generally low to medium. Measurements taken from cores in various wells in the field show that the average porosity ranges between 5% and 7%, and the horizontal permeability varies between 1 mD to 18 mD. The productive thickness in this field is approximately 50m.

Chapter III: Methods and Materials

Chapter III: Methods and Materials

I. Mechanical Earth Model (MEM) 1D Definition

A mechanical earth model (MEM) is a repository of data—measurements and models—representing the mechanical properties of rocks and fractures as well as the stresses, pressures and temperatures acting on them at depth. Engineers and geoscientists use it to understand how rocks deform, and sometimes fail, in response to drilling, completion and production operations. Each data point in an MEM is referenced to its 3D spatial coordinates and time of sample collection.

Rocks deform in a variety of ways in response to stress:

- Some rocks, such as granites, are stiff and strong.
- Some, such as mudstones, are soft and weak.
- Some, such as salts, with sufficient time can flow.

An MEM provides information about mechanical behavior and strength by using relationships between rock properties, induced deformations and ambient conditions. Because of the layered fabric of rocks or the presence of fractures, rock properties are frequently anisotropic—their properties are not the same in all directions as they would be with isotropic media.

An MEM documents the ambient conditions, including the stress, fluid pressure, temperature and fluid content, relevant for a geomechanical analysis. An MEM may represent a snapshot at a time of interest—for instance, the virgin conditions of a reservoir—or it may track how conditions evolve as the reservoir is being produced[10]

II. Components of the 1D Geomechanical Model

II.1- Stresses

The starting point for most geomechanical studies is to describe the state of in-situ stresses within the earth, which requires three magnitudes and orientation information.

In general, formations are subjected to different stresses that combine to maintain these rocks in a state of equilibrium.

II.1.1 State of Stress

The concept of stress σ\sigmaσ is simply defined as the ratio of force F to the surface area of section S.

$$\sigma = \frac{F}{S}$$

[10] SLB WebSite : https://www.slb.com/resource-library/oilfield-review/defining-series/defining-mem

Stress is therefore a force per unit area. To better represent the state of stresses, we consider a cubic element subjected to any loading. On each face, the applied force can be observed Figure 18.

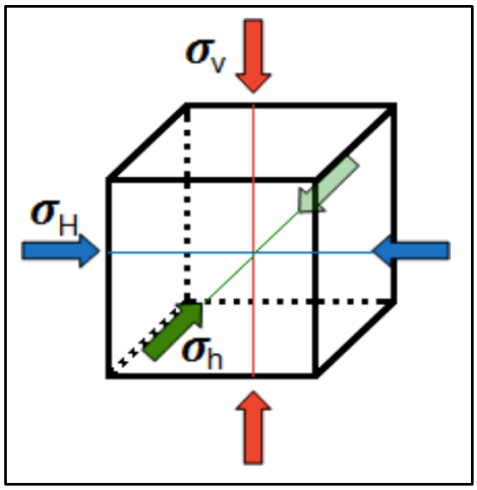

Figure 18: Principal Stresses

II.1.2 Vertical Stresses

These are mainly attributable to the masses of the formations covering the target area, from the surface to the base. In other words, it is the weight of the sediments resting on the formation. They are applied perpendicularly to the rock formation.

II.1.3 Horizontal Stresses

A horizontal stress is a shear stress applied along the surface of a plane. These stresses primarily depend on the tectonics of the area. The tectonics can have a gravitational component that can be accentuated by thermal effects, tectonic activity, and geological structure. They are subdivided into:

A. Minimum Horizontal Stress

corresponds approximately to the fracture closure pressure. The units of stress and pressure are both psi. This is not a coincidence since stress and pressure are fundamentally related. The main difference is that pressure acts equally in all directions, while stress acts only in the direction of the force. Since effective horizontal stress is a direct result of effective vertical stress, Poisson's ratio determines the amount of stress that can be transmitted horizontally. The minimum horizontal stress or fracture closure pressure can be obtained from poroelastic theory.

B. Maximum Horizontal Stress

is more difficult to calculate. This section attempts to provide various approaches and methods. In very complicated conditions, such as in a region of high tectonic stresses, multiple integrated methods and approaches must be applied to mutually verify and calibrate the model.

II.1.4 Orientation of Stresses

Hydraulic fractures tend to propagate in a plane perpendicular to the minimum in-situ stress. Therefore, if the principal stresses are vertical and horizontal, a planar fracture will tend to propagate in the direction of the maximum horizontal stress.

The direction of the maximum horizontal stress can be determined in many ways. Firstly, through borehole imaging. If a breakout occurs, it will be observed in the direction of the minimum horizontal stress, and if tensile fractures induced by drilling are created, they will occur in the direction of the maximum horizontal stress. The oriented caliper can also be used to detect the direction of breakouts.

II.1.5 Stress Regime

The magnitude of the three stresses determines, according to Andersson's classification, the stress regime which produces three different fault models:

Normal regime: σv > σH > σh (Figure 19.a)

Reverse regime: σH > σh > σv (Figure 19.b)

Strike-slip regime: σH > σv > σh (Figure 19.c)

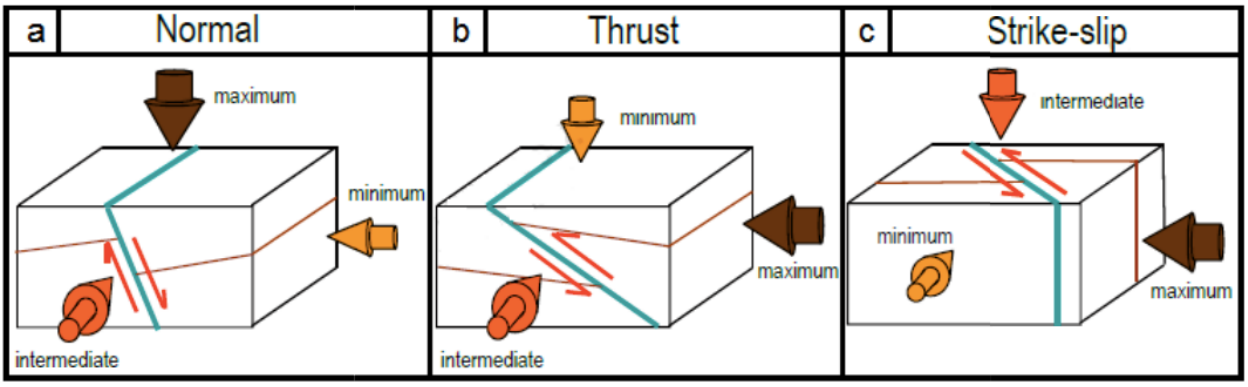

Figure 19: Fault models according to the stress regime (SLB)

II.2 Elastic Parameters of Rocks

II.2.1 Young's Modulus

It represents the ratio between the stress applied to the rock sample and the resulting deformation in the same direction as the stress Figure 20. In other words, the stiffness of a material is called Young's modulus, denoted as (E). It is characterized by the slope of the σ = f(ε) curve and depends on the elasticity, viscosity, and rigidity of the rock, as well as temperature, time, pore pressure, and anisotropy. Young's modulus is inversely proportional to deformation.

$$E = \frac{\sigma}{\varepsilon} \qquad \varepsilon = \frac{\Delta L}{L} \qquad \sigma = \frac{F}{S}$$

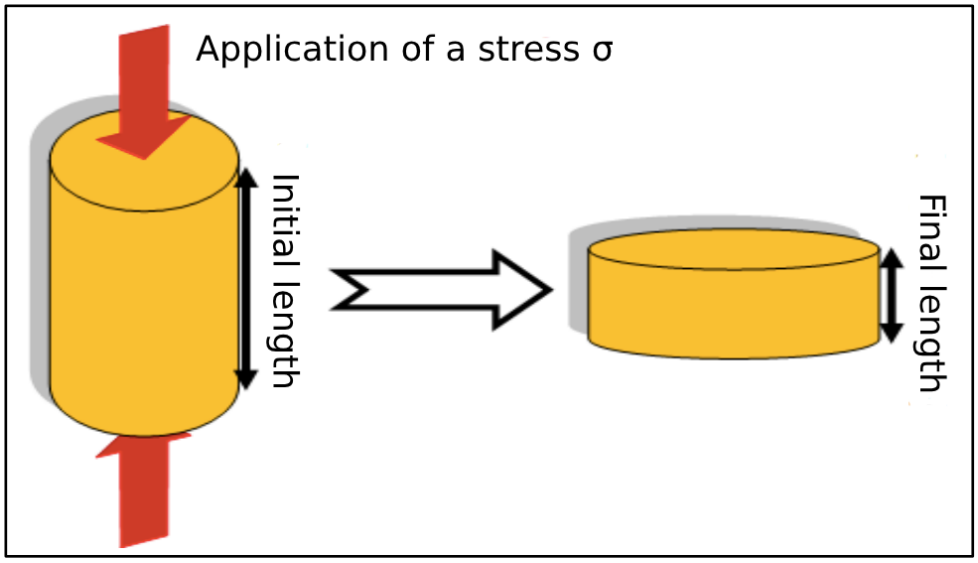

Figure 20: Deformation along a stress axis of a cylinder. (Sonatrach document, E/P division)

Note: Young's modulus varies from one rock to another. Table III.1 below presents some examples:

Rock Type	Young's Modulus (Mpsi)
Limestone	5-13
Sandstone	0.2-1.3
Consolidated Sandstone	1-8
Silt	4-8
Clay	1-5
Coal	0.1-1

Table 1: Some Examples of Young's Modulus (Sonatrach Document, E/P Division)

II.2.2- Poisson's Ratio

Poisson's ratio, represented by the symbol ν, is a dimensionless coefficient defined as the ratio of the change in lateral dimension (change in diameter, d) to the change in axial or longitudinal dimension (change in length, l) when the sample is subjected to compression (see Figure III.4). This ratio characterizes the material's contraction perpendicular to the direction of the applied force. It quantifies the variation of lateral deformation relative to axial deformation according to the following expression:

$$V = -\frac{\Delta D}{D} / \frac{\Delta L}{L}$$

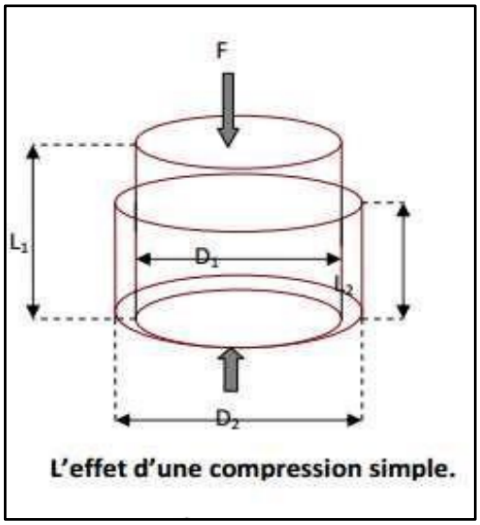

Figure 21: Lateral and axial deformations resulting from compression (Sonatrach document, E/P division)

Poisson's ratio varies from one rock to another. Table below provides some examples:

Rock Type	Young's Modulus (Mpsi)
Limestone	0.30-0.35
Sandstone	0.25-0.35
Consolidated Sandstone	0.15-0.30
Silt	0.20-0.30
Clay	0.25-0.45
Coal	0.35-0.45

Table 2: Some examples of Poisson's ratio (Sonatrach document, E/P division)

Note: The higher the Poisson's ratio, the more compressed the rock.

II.2.3- Shear Modulus

The shear modulus G is a measure of the resistance of a rock sample subjected to shear stresses; G is the ratio of shear stress to shear strain. In the English system, its unit is (MPsi: Mega Psi). It is given by the following formula :

$$G = \frac{F}{A} / \frac{\Delta X}{l}$$

where:

F is the applied force

ΔX is the lateral displacement

A is the surface area on which the force acts

l is the thickness

II.2.4 Bulk Modulus

The bulk modulus (K) is the ratio of stress under compression to the volumetric strain or the proportionality relationship between pressure and the rate of volume change. It is expressed by the following relation:

$$K = \frac{\text{Hydrostatic pressure}}{\text{Volumetric strain}}$$

It can also be expressed in terms of Young's modulus and Poisson's ratio.

II.2.5- BIOT Coefficient

The Biot elastic constant is an important poroelastic parameter of rock that describes the degree of compression of the dry skeletal framework relative to the rock matrix. This parameter ranges from nearly 0 for very rigid rocks with zero porosity (rocks containing minerals such as basalt and pyrite) to values generally close to 1 for many porous rocks in shallow sedimentary basins

II.3 Rock Strength Parameters

When a borehole is drilled, the rock strength relative to the borehole stresses determines whether the rock in the borehole walls will remain mechanically stable or undergo permanent deformation. From a strictly mechanical perspective, the necessary elements to predict stability include rock strength parameters, in situ stress, the geometry and orientation of the borehole relative to the in situ stresses, and a shear failure criterion.

The main rock strength parameters include unconfined compressive strength (UCS), tensile strength (T0), cohesion (C0), and the coefficient of internal friction (f):

- UCS is the maximum strength of the material when uniaxial compression is applied, under zero confining pressure.
- Tensile strength is the maximum strength of the material when tension is applied. Tensile strength can be measured directly on cores in the laboratory with a direct tensile test, or indirectly by Brazilian tests or bending tests.
- Cohesion and the coefficient of internal friction can be estimated by fitting uniaxial and/or triaxial compressive strengths to a Mohr-Coulomb failure envelope or other criteria.

Rock strength parameters are generally measured from core samples but can be estimated from logging data using empirical correlations.

II.4 Pore Pressure

By definition, pore pressure is the pressure exerted by the interstitial fluids within a formation. It is obtained using MDT (Modular Formation Dynamics Tester) and RDT (Reservoir Description Tool). In the absence of these tools, it can be estimated from the hydrostatic gradient using the following formula:

$$\text{PP} = \frac{TVD}{\text{The hydrostatic gradient}}$$

where: TVD is the total vertical depth.

II.5 Fracture Pressure

This is the pressure required to overcome the formation and/or open existing fractures through hydraulic fracturing. It is expressed by the following formula: $FG = \frac{\sigma_h}{TVD}$

Where: σ_h minimum horizontal stress

III. Steps for Developing a Geomechanical Model

Conducting a geomechanical study begins with the development of a 1D geomechanical model or 1D MEM (Mechanical Earth Model), which involves using data from logging and core measurements. This allows for the identification of reservoir quality and its petrophysical and geomechanical characteristics. Estimation of dynamic mechanical properties (Young's modulus and Poisson's ratio) is done through measurements of compression and shear wave velocities. Transitioning to the static regime requires the use of conversion formulas obtained through correlation with uniaxial or triaxial tests on core samples in the laboratory. Once the values of static mechanical properties are available, stress profiling is performed to determine the distribution of horizontal stresses with depth and their orientation using imaging techniques. At the end of the study, the identification of the fracturing zone is chosen after analyzing the curve of minimum stresses, which identifies the fragile intervals that allow for fracture initiation.

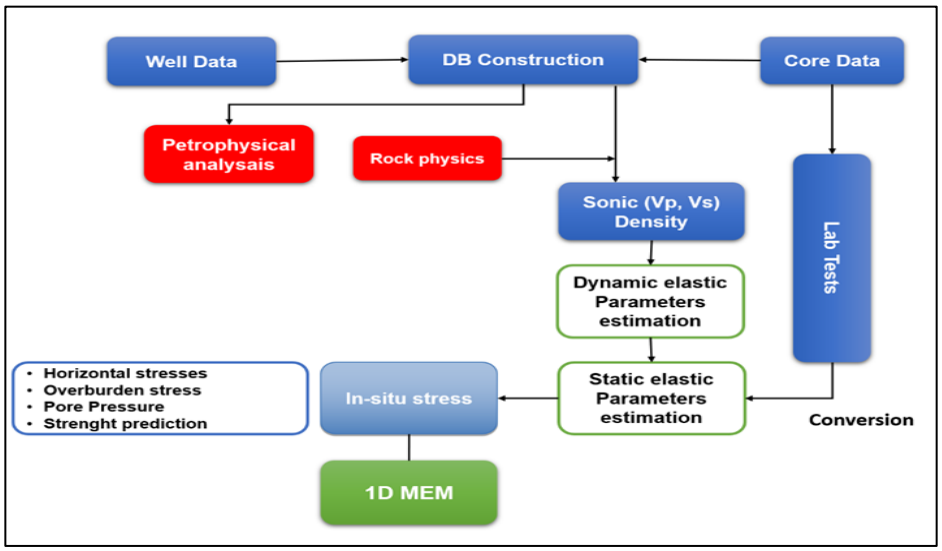

Figure 22: Mechanical Earth Model Workflow (Publication by Syofyan et al. at ADIPEC Nov'2015)

IV. Methods for Determining the Minimum Stress Zone

Determining the minimum stress zone is crucial in any hydraulic fracturing operation, as it is where the fracture will initiate. Its determination is based on the characterization of certain elastic parameters essential for calculating horizontal stresses. Therefore, to construct the 1D geomechanical model or 1D MEM (Mechanical Earth Model), it is necessary to use data from logging, mechanical tests on core samples, and well tests.

Property Profiled	Source Logs	Other Sources
Mechanical Stratigraphy	Gamma Ray, Density, Resistivity, Sonic Compressional Velocity	Cuttings, Cavings, Sequence Stratigraphy
Pore Pressure (P_p)	v_p, check-shot survey, Resistivity	Interval velocity from seismic data, formation integrity test, daily drilling reports
Overburden Stress (σ_v)	Bulk density	Cuttings
Stress direction	Oriented multiarm calipers,Borehole images	Structural maos, 3D seismic data
Min horizontal Stesss (σ_h)	v_p and sonic shear velocity v_s wireline stress tool	P_p, leak-off tests, extended leak-off tests, micro-frac, step-rate injection tests, local or regional database, daily drilling reports, modeling
Max horizontal Stesss (σ_H)	Borehole images	P_p, σ_h, rock strength, database, wellbore stress model
Elastic parameters [Young's modulus (E), shear modulus (G) Posson's ration (v)	v_p and v_s, bulk density	Database, laboratory core tests,cavings
Rock-strength parameter [unconfined compressive strength (UCS), friction angle (∅)]	v_p and v_s, bulk density mechanical stratigraphy	Database, laboratory core tests, cavings
Failure mechanisms	Borehole image, oriented multiarm caliper	daily drilling reports, cavings

Table 3: Data Required for Building MEM (Source: Master's Thesis of Leonard Knoll)

Where:

Gamma Ray (GR)

Gamma Ray logs measure the natural gamma radiation emitted by formations, primarily from uranium, thorium, and potassium isotopes. This measurement helps identify lithology, specifically distinguishing between shale (high gamma radiation) and non-shale formations like sandstone or limestone (low gamma radiation).

Source: Acquired from wireline logging tools during the well logging process.

Equations: $GR_{index} = \frac{GR - GR_{min}}{GR_{max} - GR_{min}}$

This equation normalizes the gamma ray values to help correlate shale content across different wells.

Goal: The main goal is to use the GR log to identify and quantify shale content in the formation, which is crucial for understanding the reservoir's lithology and for correlating stratigraphic units across the field.

Bulk Density (RHOB)

Bulk density measures the mass per unit volume of the formation, typically recorded in grams per cubic centimeter (g/cm³). It includes the mass of both the rock matrix and the fluids within the pore spaces.

- **Source:** Acquired using density logging tools deployed in the well.
- **Equations:** ρb=Measured Density
- **Goal:** The primary uses of bulk density are to calculate overburden stress and to derive porosity when combined with neutron porosity data. It is essential for understanding the load-bearing capacity of the formation and for geomechanical modeling.

Formation Resistivity (RT)

Measures the electrical resistivity of the formation, which varies with fluid content and type (water, oil, or gas).

- **Source:** Resistivity logging tools.
- **Equations:** $RT = a \cdot \emptyset^{-m} \cdot S_w^{-n} \cdot R_w$. (Archie's Law), where a, m, and n are empirical constants, φ is porosity, Sw is water saturation, and Rw is the resistivity of formation water.
- **Goal:** Helps in identifying fluid content and saturation, crucial for distinguishing between hydrocarbon-bearing and water-bearing zones.

Sonic Logging

Sonic logging is a well logging tool that provides valuable information about a formation's interval transit time. This transit time, denoted as Δt, measures how fast elastic seismic compressional and shear waves travel through the subsurface formations.

- **P-Waves** (Compressional Waves): Elastic deformation of grains in the direction of wave propagation.
- **S-Waves** (Shear Waves): Elastic deformation of grains perpendicular to the direction of wave propagation.

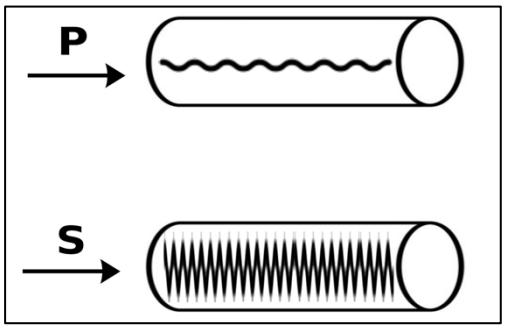

Figure 23: Modeling P and S Wave Propagation in Rocks

Caliper (CALI)

Caliper logs measure the diameter of the borehole. Variations in borehole diameter can indicate wellbore stability issues such as washouts or enlargements due to rock weakness or fracturing.

- **Source:** Obtained from caliper logging tools deployed in the well.
- **Equations:** Direct measurements of borehole diameter are used.
- **Goal:** The goal is to assess borehole conditions to detect zones of instability and ensure accurate interpretation of other logging tools that might be affected by borehole size variations.

Neutron Porosity (PHI-N)

Measures the hydrogen content in the formation, which is directly related to the formation's porosity. It is typically expressed as a percentage.

- **Source:** Neutron porosity logging tools.
- **Equations:** $\emptyset_n = \frac{Hydrogen\ Index}{Bulk\ Density}$
- **Goal:** Provides porosity values, crucial for estimating the amount of fluid-filled space in the rock, which directly affects the reservoir's capacity to store hydrocarbons.

IV.1 Calculation of Elastic Properties of Rocks

IV.1.1 Well Logs

Well logs provide input data for the MEM model by allowing direct determination of the dynamic mechanical properties of the rock and vertical stress. The log obtained from sonic logging, along with the density log, enables the calculation of reservoir elastic parameters (Young's modulus, Poisson's ratio, etc.). The two types of waves of interest for estimating the elastic constants of a medium are compression waves (P-waves) and shear waves (S-waves).

IV.1.1.1 Dynamic Measurements

Sonic waves (P and S) propagate at high frequency (10 KHz) in the formation, involving very small deformations. In this dynamic regime, rocks exhibit a stiffer response than they would under static loading during laboratory mechanical tests or static loading in the subsurface. The following mathematical equations, known as Gassmann equations, based on sonic data combined with density data, are used for the calculation of elastic parameters termed dynamic in this case.

$$G_{dyn} = (13474.45)\ \frac{\rho_z}{(\Delta t_{shear})^2}$$

$$K_{dyn} = (13474.45)_{\rho_b}\left[\frac{1}{\left(\Delta t_{comp}\right)^2}\right] - \frac{4}{3}\ G_{dyn}$$

$$E_{dyn} = \frac{9\times G_{dyn}\times K_{dyn}}{G_{dyn}+3\times K_{dyn}}$$

$$PR_{dyn} = \frac{\frac{1}{2}\left(\Delta t_{shear}/\Delta t_{comp}\right)^2 - 1}{\left(\Delta t_{shear}/\Delta t_{comp}\right)^2 - 1}$$

Where:

G_{dyn} Dynamic shear modulus (Mpsi).

K_{dyn} Dynamic bulk modulus (Mpsi).

E_{dyn} Dynamic Young's modulus.

PR_{dyn} Dynamic Poisson's ratio.

ρ_z Formation density (g/cc).

Δt_{shear} Shear sonic wave transit time (µs/ft).

Δt_{comp}Compression sonic wave transit time (µs/ft).

IV.1.2 Laboratory Measurements

These are mechanical tests conducted in the laboratory for the purpose of:

- Measuring the rock's strength (simple (uniaxial) compression and tension)
- Determining the static and dynamic elastic mechanical properties of the rock.
- Developing dynamic-static correlations.
- Determining the rock's plastic mechanical properties.

IV.1.2.1 Static Measurements

The elastic properties of the rock are calculated using the Gassmann equations, but the obtained values are overestimated because the rock exhibits a stiffer behavior, meaning the elastic properties of the rock are modified by drilling operations, and their measurements are then referred to as dynamic measurements. Therefore, it becomes necessary to resort to conversion models that allow for the transition from the dynamic regime to the static regime. However, the choice of model depends on the geomechanical behavior of the traversed formations and must be developed based on laboratory tests.

Obtaining static measurements is ensured by correlations determined by comparing static elastic properties with dynamic elastic properties. Generally, correlations take the following form:

$$Static = (A \times Dyamic^{\alpha}) + B$$

Where:

$Static$: The corresponding static elastic property

$Dyamic$: The corresponding dynamic elastic property

A and B: Determined constants

α: Biot constant, typically taken as equal to 1.

A. Static Young's Modulus

After conversion, the value of the static Young's modulus tends to decrease and shows a significant difference from the dynamic Young's modulus, hence the necessity of conversion.

For the conversion from dynamic Young's modulus to static Young's modulus, several equations are available in the literature. However, the most commonly used equations in Algeria are the Morales equation and some equations specific to service companies (e.g., Schlumberger).

It is worth noting that the difference between the two static and dynamic Young's moduli is more significant in sandstones than in carbonates.

Morales Equation: used for sandstones with porosity 10% - 15%

$$Log\ (E_{Stat}) = 2.137 + 0.6612 \log(E_{dyn})$$

Where:

E_{dyn}: Dynamic Young's modulus in Mpsi.

E_{Stat}: Static Young's modulus in Mpsi.

B. Static Poisson's Ratio

The dynamic Poisson's ratio is calculated using the Gassmann equation, while the static Poisson's ratio can be determined through core tests. Many tests have shown that the dynamic Poisson's ratio is practically equal to the static Poisson's ratio (Burstein and Frankel, 1968).

IV.2 Calculation of Pore Pressure and Stresses

The stress profile is essential for understanding the behavior and stability of the borehole. It provides information about:

- Vertical stress (Sv: Vertical Stress).
- Pore pressure (PP: Pore Pressure).
- Minimum and maximum horizontal stresses (Shmin and Shmax) as well as their magnitudes.

IV.2.1 Calculation of Vertical Stress

This is the pressure exerted at any given time by the mass of overlying sediments and fluids. It is given by the following formula: $\sigma_v = TVD \times \rho \times g$

Where:

TVD: True Vertical Depth.

g: Gravity.

ρ: Density.

IV.2.2 Calculation of Pore Pressure

Several techniques for pore pressure determination are already in use, but one of the most popular methods has been designed by the Eaton method. These equations for pore pressure can be derived from the use of well logs or seismic data.

Eaton (slowness, velocity, or resistivity): This method is one of the most widely used techniques for estimating pore pressure in the industry. It is based on Eaton's work in the Gulf of Mexico. The Eaton method utilizes a semi-logarithmic or linear trend line. The different log measurements (R) used by the Eaton method are resistivity, Sonic, or seismic velocity.

$$P_P = \sigma_v - (\sigma_v - P_{pnorm}) \times a \times \left(\frac{R}{R_{norm}}\right)^n$$

IV.2.3 Calculation of Horizontal Stresses

The poroelastic model of horizontal deformations is the most commonly used method for estimating horizontal stresses, taking into consideration tectonic effects to quantify the magnitudes of minimum and maximum horizontal stresses (Fjaer et al., 1992).

The ε_H and ε_h cannot be directly measured. By adjusting these deformations, you can calibrate the calculated stresses with the Leak-off test.

$$\sigma_h = \frac{v}{1-v}(\sigma_v - \alpha PP) + \alpha PP + \frac{E}{1-v^2}\varepsilon_h + \frac{vE}{1-v^2}\varepsilon_H$$

$$\sigma_H = \frac{v}{1-v}(\sigma_v - \alpha PP) + \alpha PP + \frac{vE}{1-v^2}\varepsilon_h + \frac{E}{1-v^2}\varepsilon_H$$

Where:

σ_h: Minimum horizontal stress.

σH: Maximum vertical stress.

ν: Poisson's ratio.

E: Young's modulus.

εH and εh: Minimum and maximum strains, respectively.

α: Biot constant (α=1 under rupture conditions).

IV.2.4 Calculation of Stresses Around the Wellbore

Before excavation, the rock formation typically maintains a state of equilibrium with minimal or no movement, assuming no nearby seismic activity. This state is characterized by three principal stresses known as in situ stresses, as outlined. However, excavation disrupts this static stress equilibrium, leading to instability in the rock formation. Consequently, a new stress regime is imposed within the excavation zone, necessitating the identification of this stress state as the initial step in analyzing formation stability.

We assume that the primary in situ stresses, σv, σH, and σh, serve as input stresses. Considering that a borehole can assume any orientation, these stresses require transformation into a new Cartesian coordinate system (x, y, z), enabling the determination of stresses σx, σy, and σz. The orientation of these new stresses is determined by the wellbore's inclination from the vertical (γ), the geographical azimuth (ϕ), and the wellbore's position from the x-axis (θ), as illustrated in Figure 24.

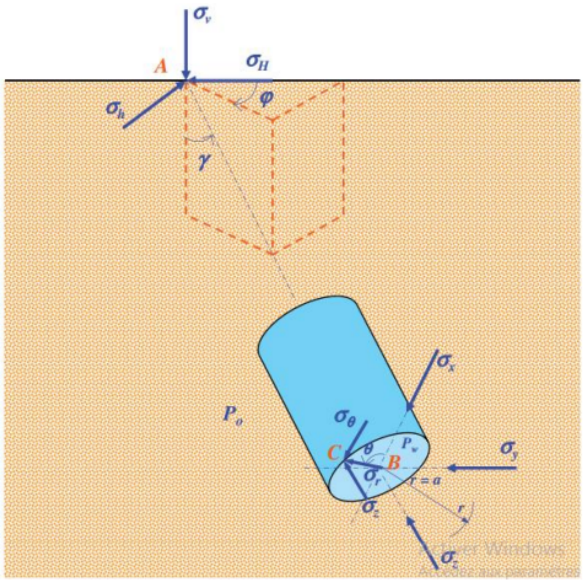

Figure 24: Stress Distribution around a Wellbore in the Rock Formation: (σv, σH, σh) denotes the in situ stress state, while (σx, σy, σz) and (σr, σθ, σz) represent stress states at the wellbore in Cartesian and cylindrical coordinate systems, respectively.

The following equations define all the transformed stress components as defined above and illustrated in the figure:

$$\sigma_x = (\sigma_H \cos^2\varphi + \sigma_h \sin^2\varphi)\cos^2\gamma + \sigma_v \sin^2\gamma$$

$$\sigma_\gamma = \sigma_H \sin^2\varphi + \sigma_h \cos^2\varphi$$

$$\sigma_{zz} = (\sigma_H \cos^2\varphi + \sigma_h \sin^2\varphi)\sin^2\gamma + \sigma_v \cos^2\gamma$$

$$\tau_{x\gamma} = \frac{1}{2}(\sigma_h - \sigma_H)sin2\varphi cos\gamma$$

$$\tau_{xz} = \frac{1}{2}(\sigma_H \cos^2\varphi + \sigma_h \sin^2\varphi - \sigma_v)sin2\gamma$$

$$\tau_{\gamma z} = \frac{1}{2}(\sigma_h - \sigma_H)sin2\varphi cos\gamma$$

The set of equations below is known as Kirsch equations (Kirsch, 1898). Sometimes, only the tangential stress component of the equation is referred to as Kirsch equation, as Kirsch (1898) first published the hoop stress acting on a circular hole.

$$\sigma_r = \frac{1}{2}(\sigma_x + \sigma_y)\left(1 - \frac{a^2}{r^2}\right) + \frac{1}{2}(\sigma_x - \sigma_y)\left(1 + 3\frac{a^4}{r^4} - 4\frac{a^2}{r^2}\right)\cos 2\theta$$
$$+ \tau_{xy}\left(1 + 3\frac{a^4}{r^4} - 4\frac{a^2}{r^2}\right)\sin 2\theta + \frac{a^2}{r^2}P_w$$
$$\sigma_\theta = \frac{1}{2}(\sigma_x + \sigma_y)\left(1 + \frac{a^2}{r^2}\right) - \frac{1}{2}(\sigma_x - \sigma_y)\left(1 + 3\frac{a^4}{r^4}\right)\cos 2\theta$$
$$- \tau_{xy}\left(1 + 3\frac{a^4}{r^4}\right)\sin 2\theta - P_w\frac{a^2}{r^2}$$
$$\sigma_z = \sigma_{zz} - 2\nu(\sigma_x - \sigma_y)\frac{a^2}{r^2}\cos 2\theta - 4\nu\tau_{xy}\frac{a^2}{r^2}\sin 2\theta \rightarrow \textit{Plane Strain}$$
$$\sigma_z = \sigma_{zz} \rightarrow \textit{Plane Stress}$$

In the case of a vertical well, we reduce the equation to finally have it in the following form:

$$P_{BD} = \left[(3 \times \sigma h) - (\sigma H) - \left(P_p\right) + (T_0)\right]$$

$$P_{BO} = \frac{\left(3 \times \sigma H - \sigma h - P_p\,(1 - N)\right) - UCS_{(psi)}}{(1 + N)}$$

Where:

$\boldsymbol{P_{BD}}$ **= breakdown pressure:** The pressure at which the rock matrix of an exposed formation fractures and allows fluid to be injected. The breakdown pressure is established before determining reservoir treatment parameters. Hydraulic fracturing operations are conducted above the breakdown pressure, while matrix stimulation treatments are performed with the treatment pressure safely below the breakdown pressure. [11]

$\boldsymbol{P_{BO}}$ **: Break Out pressure:** Break Out Pressure is the minimum pressure required to initiate and propagate fractures in the rock surrounding the wellbore. It is an important measure in both drilling operations and hydraulic fracturing[12].

IV.2.5 Orientation of Horizontal Stresses

The fracture generated propagates parallel to the axis of maximum horizontal stress (σ_H) and opens perpendicular to the axis of minimum horizontal stress (σ_h) Figure 25.

[11] SLB website : https://glossary.slb.com/en/terms/b/breakdown_pressure
[12] Society of Petroleum Engineers (SPE). (2007). *Petroleum Engineering Handbook: Volume II - Drilling Engineering*. Richardson, TX: Society of Petroleum Engineers.

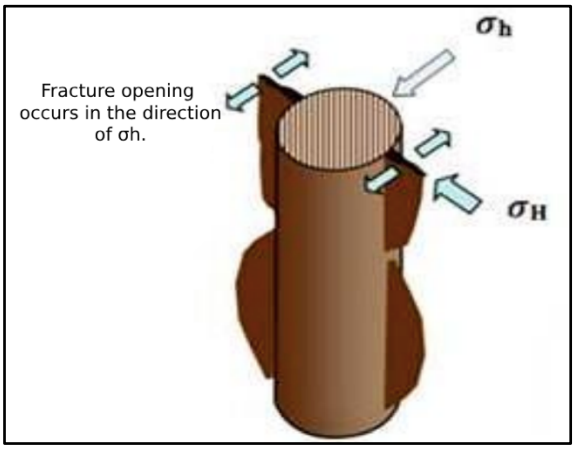

Figure 25: Fracture opening relative to horizontal stresses.

The orientation of maximum (σ_H) and minimum (σ_h) horizontal stresses can be deduced from regional tectonics, much like insights obtained from Caliper (Diameter) logs or borehole imaging, which reveal borehole ovalization Figure 26.

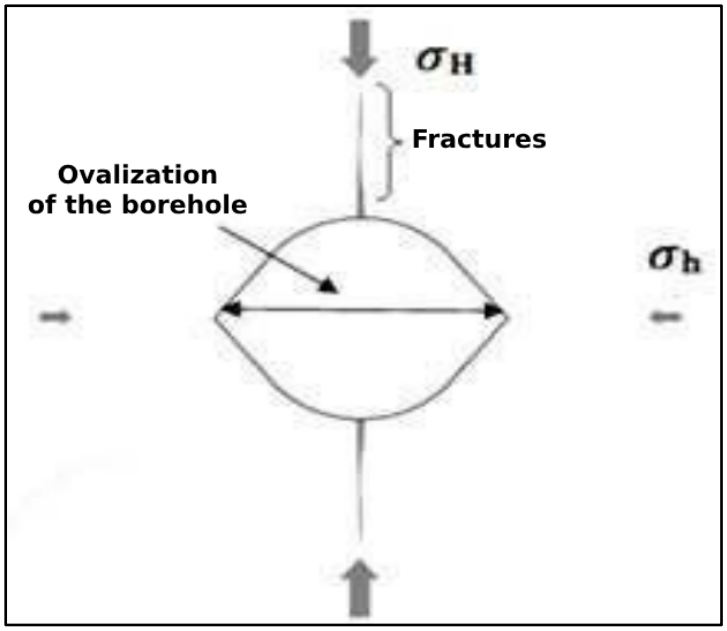

Figure 26: Determination of horizontal stresses according to induced fractures and wellbore ovalization (SLB 2007)

V. Identification of the Fracture Zone

By integrating all the utilized data and establishing the stress profile, fracture zones are selected based on several criteria, including:

- Identifying areas of minimum stress (weak zones).
- Presence of stress barriers to confine fracture propagation towards adjacent zones containing undesirable fluids.

VI. Wellbore Stability

Wellbore stability is the ability of the drilled wellbore to withstand the mechanical stresses and pressures exerted by the surrounding rock formations and drilling fluids without experiencing significant deformation, collapse, or fracturing.

Maintaining wellbore stability is critical for:

1. Safe Drilling Operations: Preventing wellbore collapse or stuck drill pipes ensures the safety of drilling operations.
2. Operational Efficiency: Stable wellbores reduce non-productive time (NPT) associated with remedial operations like sidetracking or wellbore strengthening.
3. Cost Management: Reducing the risks of wellbore instability minimizes the costs associated with lost equipment, additional materials, and extended drilling time.
4. Reservoir Access: A stable wellbore ensures effective access to the reservoir, maximizing the potential for hydrocarbon extraction.

VI.1 Factors Influencing Wellbore Stability

1. In-Situ Stresses: The natural stresses present in the rock formations surrounding the wellbore. These include vertical stress due to the weight of overlying formations and horizontal stresses from tectonic forces.
2. Rock Properties: The mechanical properties of the rock, such as compressive strength, tensile strength, porosity, and permeability, influence its stability.
3. Mud Weight and Composition: The density and composition of the drilling fluid (mud) affect the pressure exerted on the wellbore walls. Proper mud weight helps balance formation pressures and prevents influxes or blowouts.
4. Drilling Techniques: The rate of penetration, rotational speed, and other drilling parameters can impact wellbore stability. Proper control and optimization of these parameters are necessary.
5. Wellbore Geometry: The diameter, shape, and trajectory of the wellbore affect its stability. Deviated and horizontal wells may experience different stability challenges compared to vertical wells.

6. Temperature and Chemical Effects: Temperature changes and chemical interactions between the drilling fluid and the formation can alter rock properties and stability.

VI.2 Maintaining Wellbore Stability

1. Proper Mud Weight: Selecting the appropriate mud weight to balance formation pressures is crucial. Too low a mud weight can lead to wellbore collapse, while too high a mud weight can fracture the formation.
2. Monitoring and Modeling: Continuous monitoring of wellbore conditions and using modeling techniques to predict and mitigate stability issues.
3. Casing and Liner Programs: Installing casings and liners to support the wellbore walls and isolate problematic formations.
4. Managed Pressure Drilling (MPD): Using MPD techniques to precisely control the annular pressure profile within the wellbore.
5. Geomechanical Analysis: Conducting geomechanical studies to understand the stress regime and rock properties, enabling better planning and execution of drilling operations.

VII. Mud Weight

Mud weight, also known as drilling fluid density, measures the mass of the drilling fluid per unit volume. It's typically expressed in pounds per gallon (lb/gal or ppg), kilograms per liter (kg/L), or specific gravity (SG).

Importance in Drilling Operations

1. Pressure Control: Mud weight controls the pressure exerted by the drilling fluid in the wellbore, balancing formation pressures.
2. Wellbore Stability: It helps maintain wellbore stability by supporting the wellbore walls to prevent collapse or fracturing.
3. Preventing Blowouts: Sufficient mud weight prevents formation fluid influx (kicks) into the wellbore, reducing blowout risk.
4. Cuttings Transport: The density of the drilling fluid aids in carrying drilled cuttings to the surface, keeping the wellbore clean.

Determining Mud Weight

1. Formation Pressure: The required mud weight must counterbalance formation pressures.
2. Fracture Gradient: Mud weight should be below the fracture gradient to avoid wellbore fractures.
3. Well Depth and Geometry: These factors affect the hydrostatic pressure exerted by the drilling fluid column.

4. Rock and Fluid Properties: These properties influence the appropriate mud weight selection.

Adjusting Mud Weight

1. Adding Solids: Increase mud weight by adding weighting agents like barite.
2. Dilution: Reduce mud weight by diluting with base fluid or lighter additives.
3. Continuous Monitoring: Mud weight is monitored and adjusted in real-time during drilling.

Practical Applications

1. Well Planning: Engineers estimate required mud weight based on expected formation pressures.
2. Real-Time Adjustments: Mud weight is controlled and adjusted to respond to changing conditions during drilling.
3. Safety Protocols: Proper mud weight management prevents well control incidents, such as kicks and blowouts.

Challenges

1. Narrow Pressure Window: Precise control is needed in formations with narrow pressure windows.
2. Changing Conditions: Different formations require frequent adjustments to mud weight.
3. Environmental Considerations: Selection and handling of weighting agents must consider environmental impacts.

VIII. Software Used

VIII.1 Microsoft Excel

Microsoft Excel, a spreadsheet software, played a fundamental role in data entry and management. The well-log data files were initially processed using this software. It was utilized for various calculations (such as the Morales method) and to ensure compatibility with digital and graphical illustrations, as well as integration with Techlog.

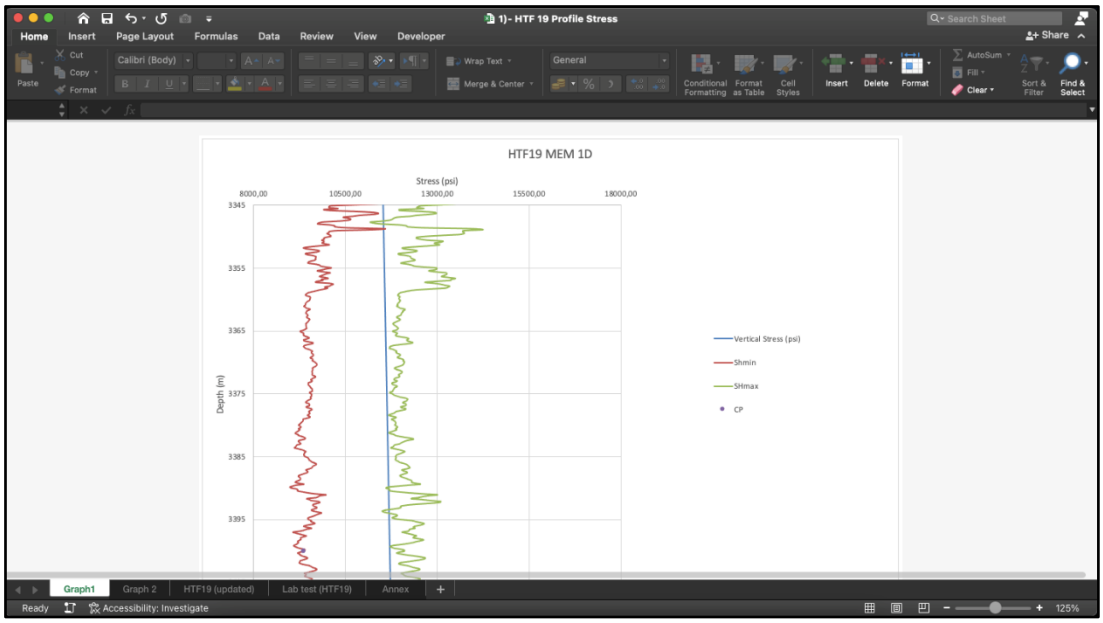

Figure 27: Interface of Microsoft Excel Software

VIII.2 Techlog Software

SLB, the world's leading provider of technology, integrated project management solutions, and information for the oil and gas industry, introduced Techlog. This platform consolidates all well information in one place.

Techlog software incorporates several crucial modules for the oil industry, including geology, geomechanics, petrophysics, drilling, and geophysics.

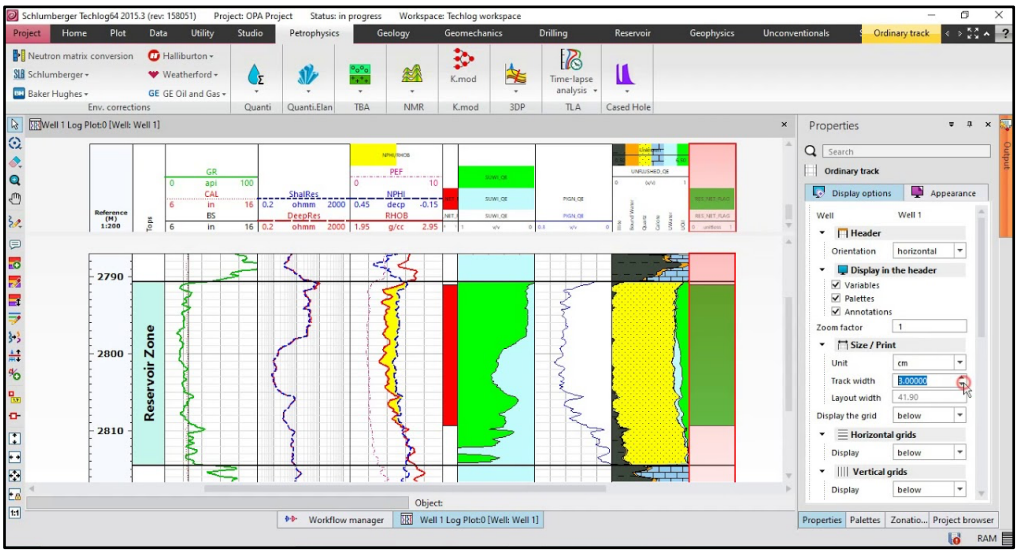

Figure 28: Interface of Techlog Software

IX. Conclusion

The significance of geomechanics in hydraulic fracturing programs cannot be overstated. By synthesizing diverse elastic and mechanical parameters of the target formation, a stress profile emerges, illuminating areas of minimal stress. These zones, crucial for fracturing, offer valuable insights into the optimal locations for effective reservoir stimulation. Thus, the integration of geomechanical principles enhances the precision and success of hydraulic fracturing endeavors, ultimately contributing to the advancement of reservoir engineering practices.

Chapter III: Practical part

Chapter III:

Practical part

I. Introduction

This chapter presents a geomechanical analysis of well HTF-19 using available data. Firstly, we will evaluate the outcomes of each component of the 1D geomechanical model derived from the methods discussed in preceding chapters. Subsequently, we will compute the in-situ stress variations relative to deviations in the angle and azimuth. Finally, we will interpret the model findings and delineate zones of minimal stress to guide the selection of fracturing locations.

I've made some adjustments for clarity and flow while maintaining the technical accuracy of the content.

II. Study Objective

This study aims to evaluate the formation's elastic properties and in-situ stresses necessary for hydraulic fracturing designs. We have chosen HTF-19 for analysis.

The primary objectives of this integrated study are as follows:

- Assess rock properties by incorporating wireline data and mechanical lab tests.
- Build 1D geomechanics model in order to estimate the in-situ stresses for the well HTF-19
- Conduct wellbore stability analysis to verify stress profiles, and regimes, and validate the MEM.

III. Mechanical Earth Model 1D Workflow

Figure 28 outlines a simplified workflow for constructing a Mechanical Earth Model (MEM). The essential stages of MEM construction, along with data integration, are elaborated upon in subsequent sections.

The typical workflow for MEM construction begins with data preparation and quality control (QC). Subsequently, the MEM construction mainly starts with the establishment of mechanical stratigraphy, followed by the calculation of elastic properties and rock strength. Next, "pressures" are computed, encompassing overburden load, pore pressure, and horizontal stresses. The final phase of MEM entails replicating observed wellbore failures using borehole imaging techniques such as FMI/OMRI or caliper logs to estimate the stress state causing these failures.

Although the primary objective of the study is stress evaluation, wellbore stability analysis is conducted as a calibration step. Following the completion of hydraulic fracturing, the model can be updated by incorporating the measured fracture gradients and acquired temperature logs.

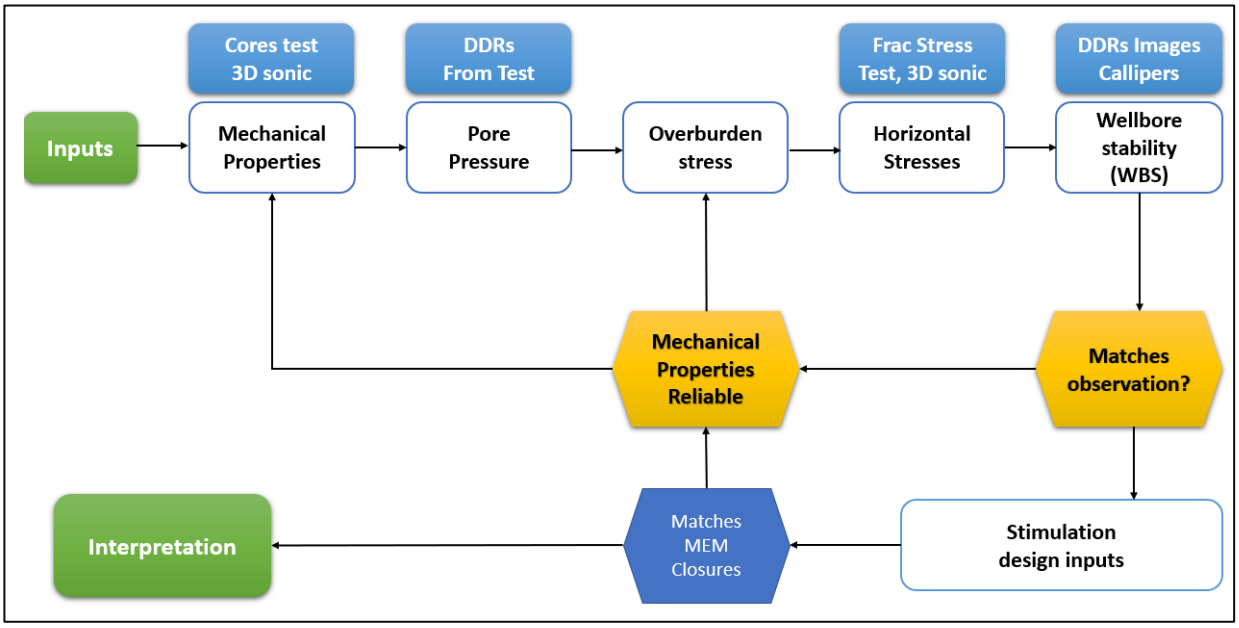

Figure 29: The Mechanical Earth Model Workflow (SLB /HTF-19 Report)

This workflow is mainly based on several steps conducted to build 1D geomechnical model. The main steps are defined as follows:

- Data collection,
- Mechanical properties calculations,
- Pore pressure estimation,
- Overburden stress estimation,
- Minimum horizontal stress estimation,
- Maximum horizontal stress estimation and finally,
- Wellbore stability analysis.

The different data collected will be checked and analysed in order to have an overview about the available and the missing data, and their reliability. They could be related to different aspects such as seismic, geology, drilling, logging, laboratory (core data), well test, frac data and others. They will be imported into the system (created through analysis or created manually by the engineers) and will be firstly used to calculate the different mechanical properties of formations. Secondly, the estimation of pore pressure by using the available models or the well test data. After that, the overburden stress estimation will be run by mainly using rock bulk density dataset. Furthermore, having rock mechanical properties, pore pressure and overburden stress will lead to the estimation of both minimum and maximum horizontal stresses and finally, running wellbore stability analysis to get a final calibrated model.

III.1 Main data used and data Audit

The initial phase of this study involved a data audit to assess data quality and suitability and to identify any potential data gaps that could introduce uncertainty into subsequent analyses. All available data of well HTF19 were reviewed to evaluate the quality of input data.

The dataset provided exhibits good quality for HTF-19. Core test results necessary for rock properties calibration are accessible for HTF-19, including UCS (unconfined compressive strength) from plug and scratch tests, as well as measurements of rock elastic properties. Compressional and shear slowness, along with density measurements, are available[13]. It's noteworthy that the quality of the wellbore, as indicated by Caliper logs, positively influenced the quality of wireline logs, particularly density logs, which are sensitive to poor hole conditions.

The available data for the study listed as follows:

- **Logging Data:** Gamma Ray (GR), Caliper (CALI), DT- Compressional, DT-Shear, Bulk Density, Neutron Porosity, Formation Resistivity, Porosity, Permeability, Water Saturation, ELAN Volumes/VCL, and Image Logs (OMRI)
- **Core data:** UCS, dynamic and static elastic properties, slowness and correlations.
- **Drilling:** DDRs
- **Well test data:** Pressure Measurements (DST)
- **Frac data:** Closure pressure

IV. Geomechanics model construction (MEM 1D)

The first step of modelling is to introduce the inputs data into the software in order to bluid all the needed data and models to give ability to engineers to analyse, study and asses the problem and try to find and recommend the best solutions for the case.

The data listed earlier have been used to build the 1D MEM of the well HTF-19 following the main steps presented in the workflow presented above.

IV.1 Rock Mechanical Properties Computation

The rock mechanical properties include elastic properties such as Young's modulus (E) and Poisson's ratio (PR), as well as rock strength properties like unconfined compressive strength (UCS), tensile strength (TSTR), and internal friction angle (FANG). Log data, notably compressional and shear slowness, and bulk density are utilized to determine these properties.

Rock mechanics testing results are incorporated into the model to refine the rock mechanical properties from logs, reducing uncertainties in rock elastic properties and strength parameters and enhancing the reliability of subsequent calculations. The mechanical core dataset of two wells (HTF-10 and HTF-19) were used, both showing consistent rock properties within the Hamra Quartzite reservoir.

III.3 Mechanical Elastic Properties

Isotropic dynamic elastic properties can be directly determined from sonic and density data using the following equations (Gassmann, 1951):

[13] 1D Geomechanics modelling for hydraulic fracturing design in Hassi Tarfa field (SLB SIS-Data Services)

$$G_{dyn} = (13474.45)\frac{\rho_b}{(\Delta t_{shear})^2} \quad (1)$$

$$K_{dyn} = (13474.45)_{\rho_b}\left[\frac{1}{(\Delta t_{comp})^2}\right] - \frac{4}{3}G_{dyn} \quad (2)$$

$$E_{dyn} = \frac{9\times G_{dyn}\times K_{dyn}}{G_{dyn}+3\times K_{dyn}} \quad (3)$$

$$PR_{dyn} = \frac{\frac{1}{2}\left(\Delta t_{shear}/\Delta t_{comp}\right)^2 - 1}{\left(\Delta t_{shear}/\Delta t_{comp}\right)^2 - 1} \quad (4)$$

Where:

$\boldsymbol{G_{dyn}}$ is dynamic shear modulus in M psi, $\mathbf{K_{dyn}}$ is dynamic bulk modulus in M psi, $\boldsymbol{\rho}$ is bulk density in g/cc, $\boldsymbol{E_{dyn}}$ is dynamic Young's modulus and $\boldsymbol{PR_{dyn}}$ is dynamic Poisson's ratio; $\boldsymbol{\Delta t_{shear}}$ and $\boldsymbol{\Delta t_{comp}}$ are shear slowness and compressional slowness (both in µs/ft), respectively.

The elastic properties obtained from Equations (1), (2), (3), and (4) are referred to as dynamic properties because the measurements are conducted at very high frequencies (around 10 kHz), involving very small strains, and the formations exhibit essentially an undrained response. Under these dynamic conditions, rocks display a stiffer response compared to static loading scenarios, such as laboratory compression tests or static loading near a wellbore or completion. In fact, the weaker and more flexible the rock, the greater the differences between dynamic and static properties. Since wellbore deformation and failure occur at a relatively slower pace compared to high-frequency wave propagation, static data are essential for geomechanical analysis. The most suitable correlation for transformation is typically established from laboratory test data on cores (An example of core data result is shown on the Figure30). The figure illustrates an almost linear trend between dynamic and static Young's modulus, which is commonly observed in tight sand formations. Indeed, the ratio between the two parameters is close to 0.9, indicating tight formations.

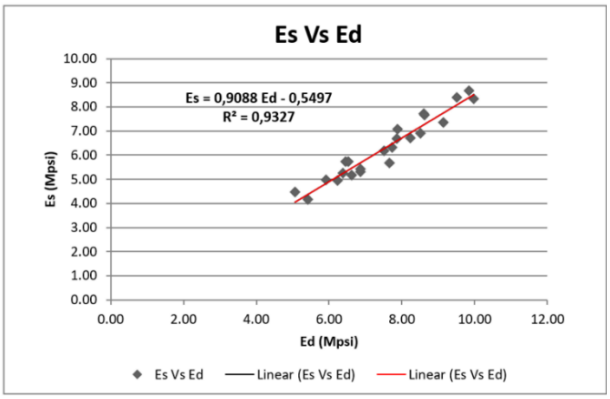

Figure 30: Static versus dynamic Young's modulus and Poisson's ratio derived from core test data of well HTF-19.

Figure 30 : Correlations derived from geomechanics core tests (HTF-19) : UCS Versus Static Young's Modules and Static Young's Modules Versus Dynamic Young's Modulus.

It's commonly assumed that the static Poisson's ratio equals the dynamic Poisson's ratio, as evidenced by various studies grounded in rock mechanics tests (Burshtein, 1968). However, from the mechanical tests we've received, no clear trend emerges between dynamic and static Poisson's ratio. Nevertheless, it appears that the dynamic Poisson's ratio is slightly higher by approximately +1 compared to the static ratio.

Typically, the core data are obtained from lab tests conducted on rock samples taken from cores. The same rock sample will be subjected to two tests, sonic (dynamic) and static. The sonic test is non-destructive test; otherwise, static test is destructive test, the sonic test is then the first test should be run before the static one.

The sonic measurements will provide slowness and dynamic elastic properties data; the static tests will give the strength and static elastic properties data. By correlating these two datasets, several correlations or models could be developed for many purposes; these correlations are called local correlations and they are the most representative correlations for the well, the reservoir or the region.

The core correlations data are mainly used for the following purposes:

- Calibrating data to reduce uncertainties into subsequent analyses and calculations,
- Completing the data profile gaps,
- Building data for new wells or missed well data,
- Deriving and developing missing data from available data,

The mechanical elastic properties calculated in the Hamra Quartzite formation through the well HTF-19 are depicted in the figure31. The mechanical elastic properties profiles are calibrated by using core data.

he description of the curves on the figure 31 from left to right is as follows:

- **Track 1:** MD: Measured Depth (m);
- **Track 2:** Stratigraphy: Formation tops;
- **Track 3:** Well Schematic
- **Track 4:** Mechanical stratigraphy: clay/shale (**green**) and sandstone (**yellow**) facies; Gamma-ray (GR, gAPI);
- **Track 5:** Bit Size & Calliper
- **Track 6-8** Input logs: Bulk Density (RHOB, g/cm3), Compressional slowness (DT, us/ft) from logs and cores; Shear slowness (DTS, us/ft) from logs and cores;
- **Track 9:** Dynamic Young's modulus (YME_STA, GPa) from logs and cores (black dots)
- **Track 10:** Dynamic Poisson's ratio (PR_Dyn) from logs and cores (black dots);
- **Track 11:** Static Poisson's ratio (PR_STAT) log compared to measurement from core tests under confinement (red dots) and unconfined (blue dots);
- **Track 12:** Static Young's modulus (YME_STA, GPa) log compared to measurement from core tests under confinement (red dots) and unconfined (blue dots);

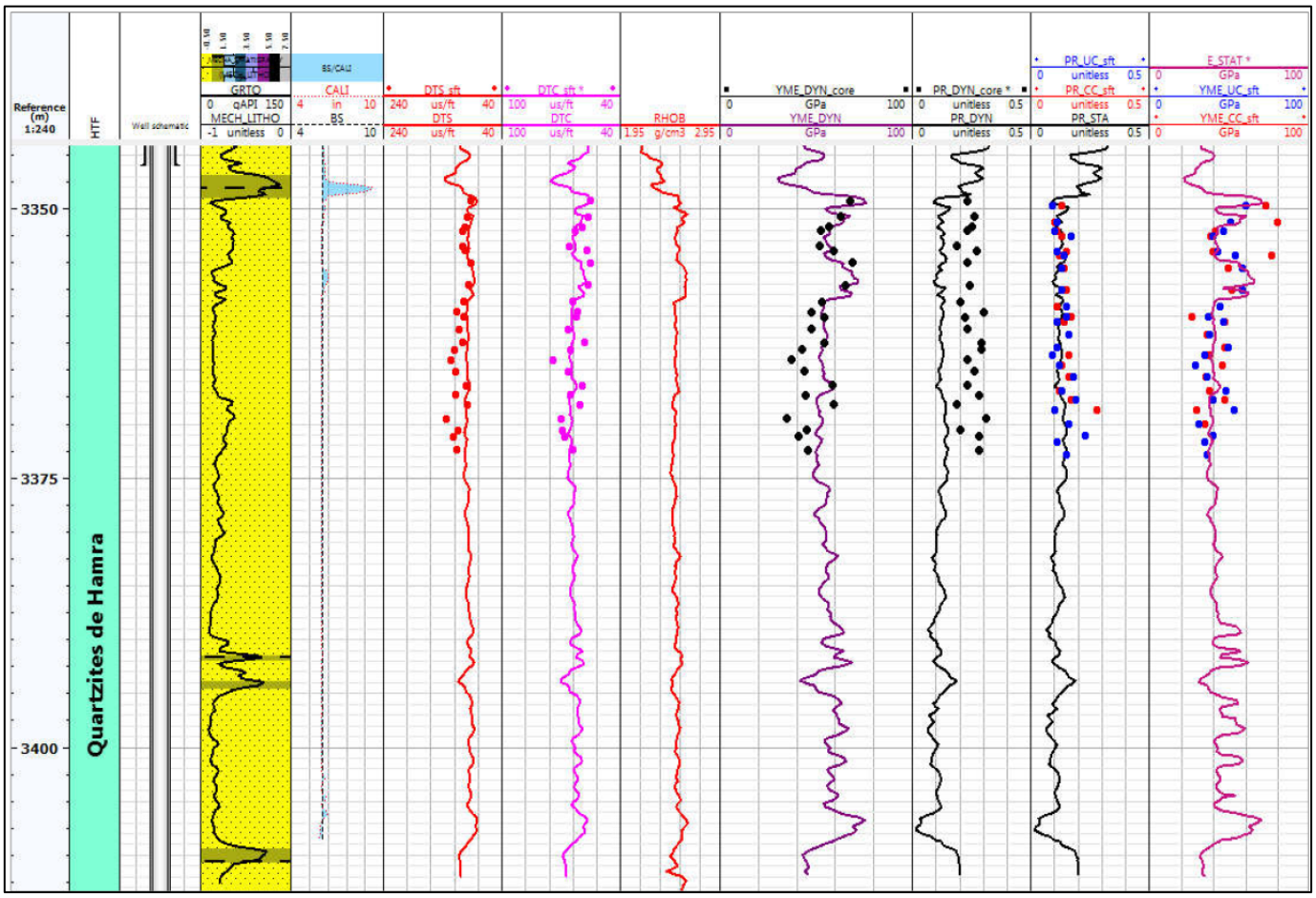

Figure 31: Rock elastic properties from logs and cores for well HTF-19. (Source: SLB SIS Data Service Report)

The comparison between logs and core measurements begins with compressional and shear slowness, which are more consistent for compressional and slightly less for shear slowness (Track 6 & 7). Shear slowness (DTS) from core appears slightly higher than that acquired from logs, especially below 3360m-. Nevertheless, comparable acoustic slowness (mainly compressional) from cores and logs suggests that the Hamra Quartzite formations may not be highly sensitive to stress.

Dynamic Young's modulus demonstrates consistent results between core and logs. Poisson's ratio is higher for cores than logs, primarily due to differences in DTS measurements. However, this discrepancy in dynamic Poisson's ratio (PR) is not observed in static parameters. It's noteworthy that static PR was assumed to be equal to the dynamically calculated value using wireline sonic data. Ultimately, static parameters (Young's modulus and Poisson's ratio) calculated using wireline and corrected based on established correlations match the static core results. It's also important to mention that both confined and unconfined static parameters from core tests display consistent results, confirming that the Hamra Quartzite is not highly stress-sensitive.

Figure 31 illustrates that Young's modulus in the Hamra Quartzite ranges from 40 to 60 GPa, with a trend of increasing towards cote 3350m. The Poisson's ratio is less variable, averaging around 0.12, with an opposing trend observed in a local shaly interval at 3347m. These results suggest that the profiles of minimum and maximum horizontal stresses are likely influenced more by Young's modulus than Poisson's ratio.

III.4 Rock Strength Computation

In addition to the rock elastic properties discussed earlier, rock strength parameters are essential for fully characterizing the mechanical response and load-bearing capacity of the rock. The Unconfined Compressive Strength (UCS) is a crucial rock property used in geomechanical analysis. To determine the UCS in the Hamra Quartzite formations, correlations with static Young's modulus and compressional slowness were developed from core data (see Figure 32). The results indicate strong correlations, particularly for the relationship between UCS and static Young's modulus (R2 = 0.86). It's important to note that this correlation incorporates data from both HTF-19 and HTF-10.

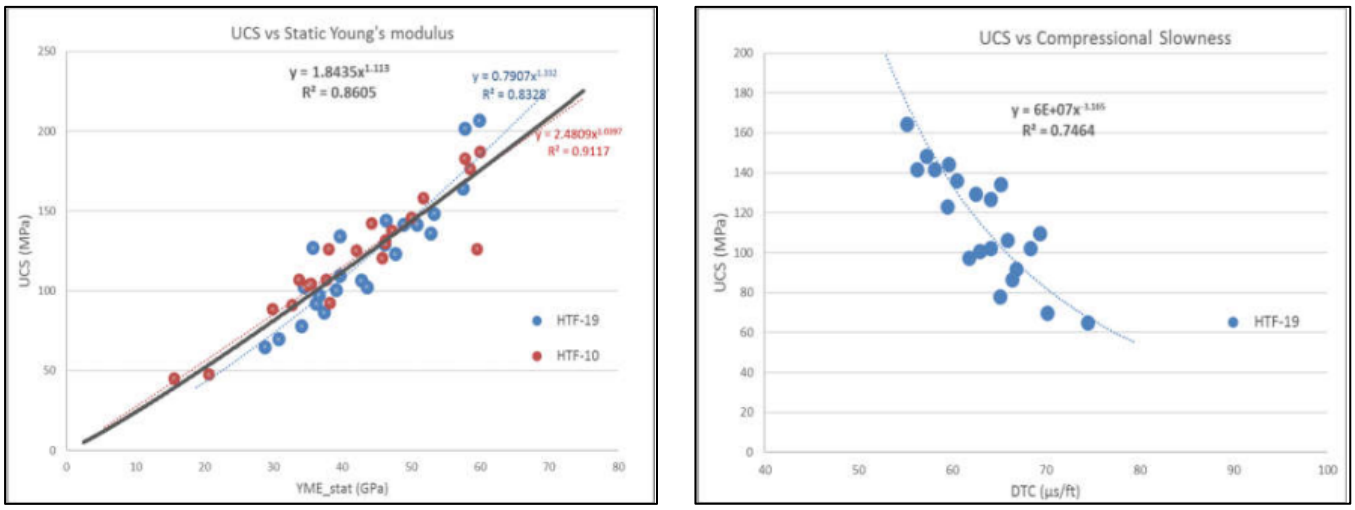

Figure 32: UCS versus static Young's modulus and compressional slowness from HTF-19 and HTF 10 core test data

The figure above shows clearly that the relationship between UCS and static Young's modulus obtained from the cores of the wells HTF-10 and HTF-19 has almost the same trend.

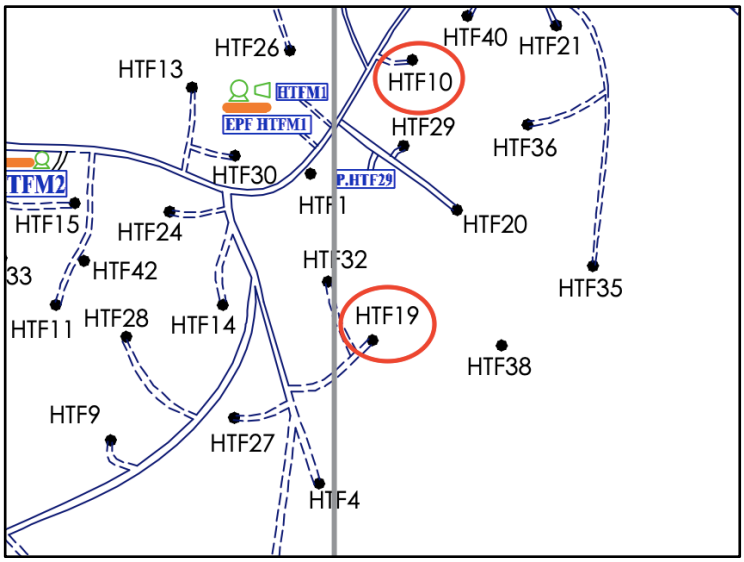

Figure 33: Location of Wells HTF19 and HTF10 in the HTF Field

The friction angle value is determined through a correlation involving the Gamma Ray (GR) or the volume of clay (V_clay), which is a standard output of ELAN results. A cut-off of 20 degrees is used for pure shale, while 45 degrees is used for pure non-shales.

The tensile strength (TSTR) of the formation is utilized to assess tensile failure of the borehole due to stress concentration. Typically, it is considered as a fraction of the Unconfined Compressive Strength (UCS) at any given point. For weaker rocks like shales, it is usually around 8-10% of UCS, while in stronger rocks, this ratio may decrease to 5-6% only[14]. In the case of HTF-10, where Brazilian tests have been conducted, the results indicate that the TSTR/UCS ratio is close to 6%.

The mechanical rock properties results of the studied well (HTF-19) are presented in Figure 34. The description of curves from left to right is as follows:

- **Track 1:** MD: Measured Depth (m);
- **Track 2:** Stratigraphy: Formation tops;
- **Track 3:** Well Schematic
- **Track 4:** Mechanical stratigraphy: clay/shale (**green**) and sandstone (**yellow**) facies; Gamma ray (GR, gAPI);
- **Track 5-6:** Input logs: Compressional slowness (DT, μs/ft); Shear slowness (DTS, us/ft); Bulk Density (RHOB,g/cm3),
- **Track 7**: Static Young's modulus (GPa) log compared to measurement from core tests under confinement (red dots) and unconfined (green dots);
- **Track 8:** Static Poisson's ratio (PR_STAT) log compared to the measurement from core tests under confinement (blue dots) and unconfined (blue dots);
- **Track 9:** Unconfined Compressive Strength UCS (MPa) compared to measurement from core tests (red dots) and scratch tests (grey dots);
- **Track 10:** Tensile Strength TSTR (MPa); Friction angle, (deg);

[14] 1D Geomechanics modelling for hydraulic fracturing design in Hassi Tarfa field (SLB - SIS-Data Services)

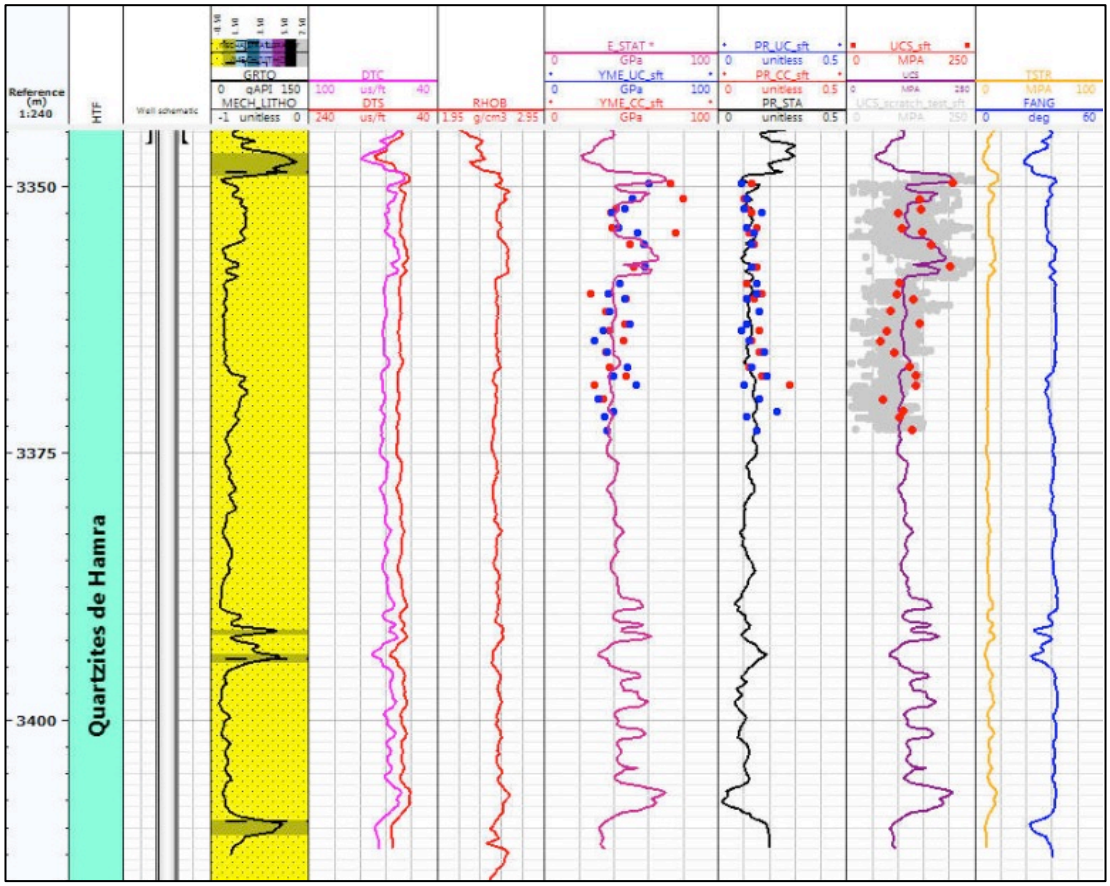

Figure 34: Rock Strength parameters from logs and cores of the well HTF-19.

From Figure 34, it's evident that the Unconfined Compressive Strength (UCS) calculated using the local correlations established earlier aligns well with the UCS measured on cores or by scratch tests. The calculation reveals that the UCS in the sandstones of the Hamra Quartzite ranges from 100 MPa to 200 MPa in certain local intervals (equivalent to 10 to 25 kPsi), with an average value of 100 MPa.

IV. In-situ Stresses and Pore Pressure

IV.1 Vertical Stress and Pore Pressure

The vertical (overburden) stress at a specific depth point beneath the ground surface is determined by the weight of the overlying earth material. It can be calculated by integrating a density log for the formations above, using the following equation (5).

$$\sigma_z = \int_0^z \rho\,(z).\,g.\,dz \qquad (5)$$

Where:
$\boldsymbol{\sigma_z}$ is overburden stress, $\boldsymbol{\rho}$ is formation density, and $\boldsymbol{g}$ is the gravitational constant.

The absence of data for certain formations and the quality of the density log can impact the accuracy of the calculated overburden stress (Dyke, 1988). In cases where density data is missing, the log is extrapolated using an exponential curve. This curve can be described by the following Equation (6):

$$\rho_b = \rho_{sur} + A_0\,.(TVD - WD - AG)^{\alpha} \qquad (6)$$

Where:

ρ_{sur} A_0 and L are three fitting parameters, TVD is true vertical depth, WD (0 in this case) is water depth and AG is air gap.

The parameters for the exponential curve are determined by adjusting the three reference points to align the exponential curve with the density log over the depth interval for which density data was available. The vertical stress profile, along with density logs, is illustrated in the Figure 35 below.

The overburden gradients for the well-chosen for our study range from 1.0 to 1.10 psi/ft, a range in close alignment with the universally accepted value of 1.0 psi/ft.

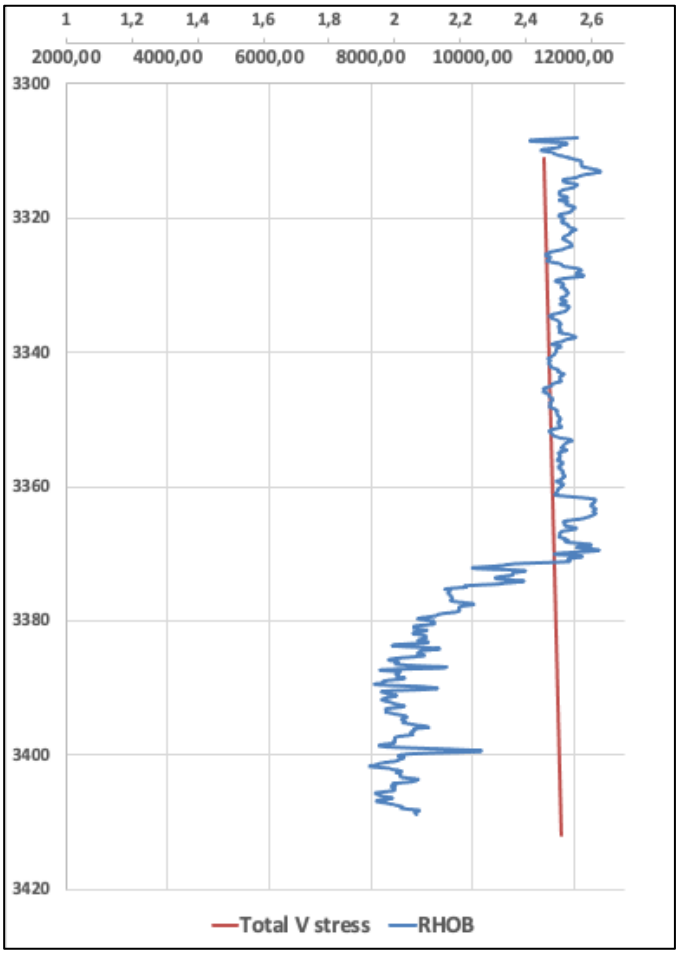

Figure 35: Overburden/vertical stress calculation for HTF-19 (Using Excel)

Pore pressure is a crucial factor in a MEM (Mechanical Earth Model) as it contributes to the total stresses exerted on a volume of rock. Therefore, it plays a vital role in the analysis of wellbore stability. Throughout the field's lifecycle, pore pressure magnitudes and fracture gradient are expected to fluctuate due to production and injection activities.

The normal or hydrostatic pore pressure can range between 1.0 sg (0.433 psi/ft, for freshwater) and 1.1 sg (0.477 psi/ft, for brine), depending on water salinity. Pore pressure estimation was conducted in the Hamra Quartzite reservoir using DST data. The measurements in HTF-19 were found to have a pore pressure gradient fluctuating around 0.55 psi/ft. This gradient serves as input for pore pressure calculations in the wells under study.

IV.2 Horizontal stress directions

Determining stress direction is often crucial in geomechanical analysis. Identifying the stress direction facilitates improvements in well trajectory design, aiming to minimize wellbore instability while considering stress anisotropy. Knowledge of stress direction also contributes to optimizing perforation, completion design, and reservoir stimulation. Various methods can be employed to identify stress direction, including failure orientation, sonic shear slowness anisotropy, and three-component Vertical Seismic Profiling (VSP).

Compressive shear failure is characterized by symmetrical hole enlargements (breakouts) aligned along the minimum horizontal stress. Conversely, drilling-induced tensile fractures (DITF), if present, occur in the direction of maximum horizontal stress.

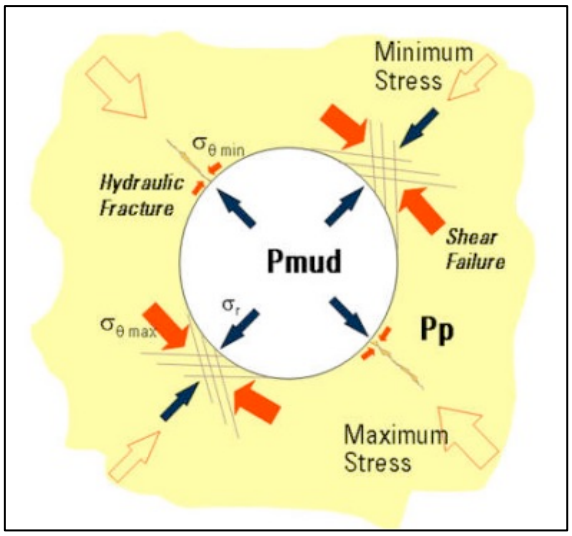

Figure 36: Distribution of horizontal stresses around a vertical wellbore and associated failures.

Depending on the relative magnitudes of horizontal principal stresses (i.e., anisotropy), along with rock strength and mud weight used during drilling, stress-induced failures may develop, with their severity varying.

Borehole images were acquired in well HTF-19 using the ECBIL tool, according to data provided. Unfortunately, these images were not processed, interpreted, or provided for the study. In the absence of information for this well, we assume that the general orientation of the minimum horizontal stress, as defined in most wells in the South of Algeria, applies to the study well. This orientation is assumed to be N030° for the minimum in-situ horizontal stress (σ_h) and N120° for the maximum horizontal stress (σ_H).

IV.3 Horizontal stress magnitudes

The poro-elastic horizontal strain (PHS) model (Fjaer et al., 1992), incorporating tectonic effects, was employed to simulate the magnitudes of the minimum (Equation 7) and maximum (Equation 8) horizontal stresses.

$$\sigma_h = \frac{v}{1\quad v}\left(\sigma_v \quad \alpha P_p\right) + \alpha P_p + \frac{E}{1\quad v^2}\,\varepsilon_h + \frac{vE}{1\quad v^2}\,\varepsilon_H \qquad (7)$$

$$\sigma_H = \frac{v}{1-v}(\sigma_v - \alpha P_p) + \alpha P_p + \frac{vE}{1-v^2}\varepsilon_h + \frac{E}{1-v^2}\varepsilon_H \qquad (8)$$

Here, the two horizontal strains, ε_h and ε_H, may exhibit either compressional or extensional behavior and can be regarded as calibration factors adjustable to align with stress-related data from leak-off tests, micro-fracturing tests, or specific rock failure modes observed in image logs, among other sources. BIOT's elastic constant α is assumed to be 1.

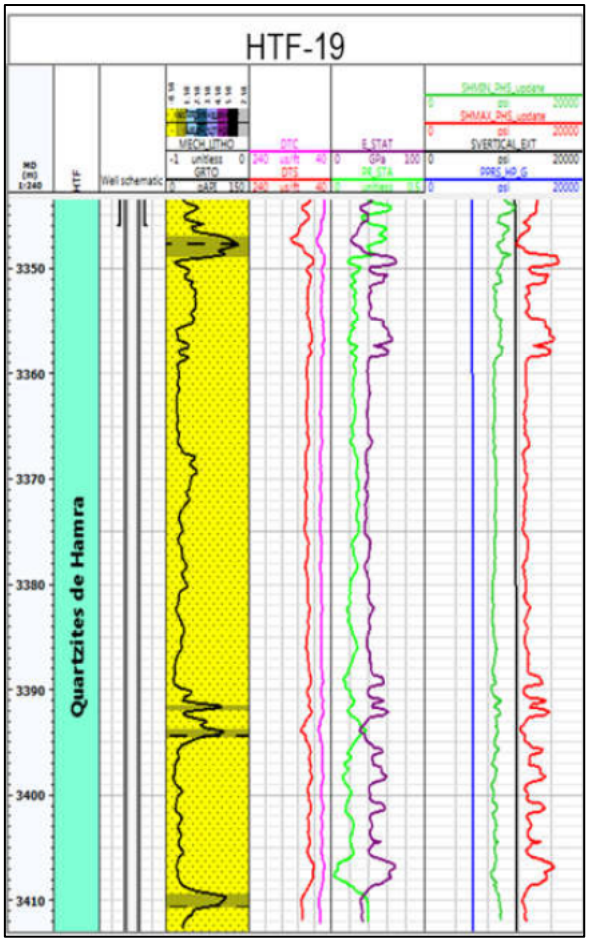

Figure 37: In-situ Stress profiles for HTF-1 9 with calibration data from injection test.

The description of curves from the left to right in Figure 37 is as follows:

- **Track 1:** MD: Measured Depth;
- **Track 2:** Stratigraphy: Formation tops;
- **Track 3:** Well Sketch;
- **Track 4**: Mechanical stratigraphy;
- **Track 5:** Compressional and shear slowness;
- **Track 6:** Static Young's modulus and Poisson's ratio;
- **Track 7:** Pore pressure (**blue**), overburden (**black**), minimum and maximum horizontal stresses (**green** and **red** logs) and closure pressure from injection test (as point data).

Minimum stress profiles from Figure 37 exhibit a similar trend to Young's modulus profiles for the well under study. Uniform profiles characterize the intervals between 3358-3390m, where the reservoir demonstrates better quality. Below this interval (below 3390m), higher variability and values are observed. In the upper part (above 3358m), the

minimum horizontal stress increases by more than 1000 psi, potentially serving as an upper barrier for hydraulic fracturing, if pursued. The combination of minimum stress profiles with high Young's modulus could present challenges for hydraulic fracturing of the Hamra Quartzite, but certainly not render it impossible. All these factors should be taken into consideration in frac design to tailor frac operations to the in-situ conditions.

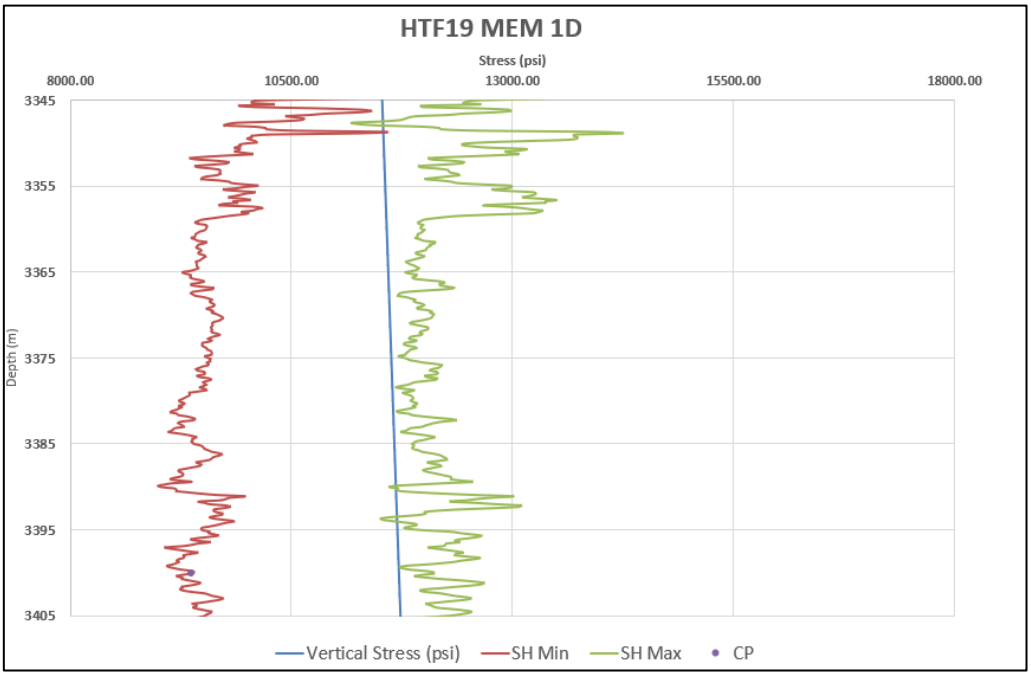

Figure 38: HTF19 MEM 1D Stress Profile Log (By Excel)

The figure above shows the variation of the three principal stresses as a function of depth for the well HTF-19. The stress magnitudes model obtained for the depth interval 3345-3405 m shows that there is one stress regime which is the strike-slip stress regime (σH > σv > σh) where the maximum horizontal stress is the higher magnitude. The vertical stress seems to be slightly less than the maximum horizontal stress especially from the depth 3360 m. The difference between the vertical and the maximum horizontal stresses for the depth interval 3345-3360 m tends to be higher than the lower part where the maximum horizontal stress shows big values. Otherwise, the minimum horizontal stress is the smallest stress with a big stress magnitude gap regarding the vertical stress magnitude, especially from the depth 3350 m. The lowest value of the minimum horizontal stress is estimated at the depth 3390 m around 8800 Psi.

The minimum horizontal stress profile has been calibrated by using ε_{min} = 0.00027 data ε_{max} = 0.0007 where the closure pressure was estimated close to 9200 Psi at the depth 3400 m (blue point on the graph).

V. Wellbore Stability

V.1 Rock Failure Criteria

The Mohr-Coulomb yield criterion utilizes the unconfined compressive strength (UCS) and the friction angle (FANG) to formulate the yield envelope.

$$\sigma_1' = UCS + \sigma_3' * tan^2\,\gamma \quad \text{where } \gamma = {}^{\pi}/_{4} + FANG/2$$

The principal stress tensor around the borehole is determined as a function of far-field principal stresses, mud weight, borehole orientation, and azimuth relative to the principal stress axes (Fjaer et al.). Using the Mohr-Coulomb criterion, one can predict the minimum mud weight required to prevent shear failure of the wellbore. This requirement will vary depending on the well orientation, as will the mud weight threshold for tensile failure.

The maximum mud weight is constrained by mud loss and hydraulic fracture gradients, which are influenced by the stresses surrounding the borehole. By comparing this mud weight to the actual mud weights utilized during drilling, it becomes possible to anticipate where borehole damage may occur. This information is utilized to calibrate geological stresses, as explained previously.

V.2 Mud Weight Window

The outcome of the wellbore stability analysis is depicted through a mud weight window. This window is delineated by four boundaries (refer to Figure 39):

1. The first boundary, starting from the left, represents the pore pressure limit. This limit should be surpassed to maintain an overbalance in the well and prevent kicks.
2. The second boundary, positioned at the lowest level, denotes the shear failure limit. Ideally, the mud weight should exceed this limit. If the mud weight drops below this threshold (indicated by red shading), compressive shear failure may occur at the wellbore wall, potentially leading to breakouts.
3. Moving upwards, the next boundary represents the mud loss gradient. This boundary is defined by the least principal stress (in this case, the minimum horizontal stress, shown in blue shading). When the mud weight surpasses this limit, mud losses can commence due to the opening of pre-existing fractures. This can result in instability in fractured formations as fractures propagate and drilling fluid is lost, causing a decrease in equivalent circulating density (ECD) or equivalent static density (ESD) during connections or tripping. Additionally, faults intersecting the well path may be reactivated if this boundary is exceeded.
4. The final boundary indicates rock tensile failure, occurring when the mud weight is excessively high. This situation puts the wellbore wall under tension, surpassing the tensile strength of the rock and leading to formation breakdown and unstable fracture propagation. Severe mud losses can arise when this pressure threshold is exceeded in intact formations.

The mud weight utilized for drilling each section is illustrated in Figure39 by a green line.

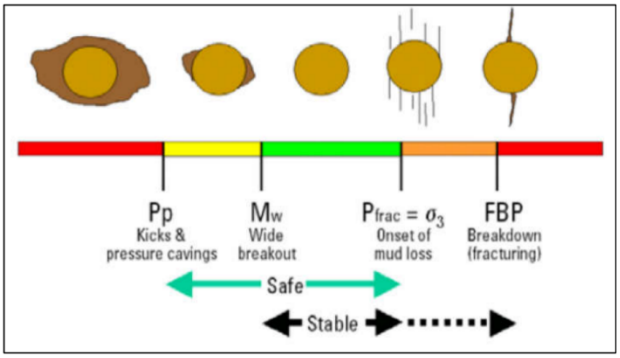

Figure 39: Wellbore Stability limits with “safe” and “stable” window to drill displayed.

The wellbore stability results for well HTF-19 are depicted in Figure 40 respectively. Here are the explanations of the curves in the different tracks in these figures (from left to right):

- **Track 1:** MD: Measured Depth (m);
- **Track 2:** Stratigraphy: Formation tops;
- **Track 3:** Well Schematic;
- **Track 4:** Mechanical stratigraphy: clay/shale (**green**), clean interval (**yellow**) facies; Gamma ray;
- **Track 5:** Static Young's modulus; Poisson's ratio (PR_STA);
- **Track 6:** In-situ stresses (psi): Pore pressure, Overburden Stress, Minimum and Maximum Horizontal Stress;
- **Track 7:** Unconfined Compressive Strength, Tensile Strength, Friction Angle;
- **Track 8:** Wellbore Stability Track including kick (gray curve), wellbore shear failure i.e. breakouts (yellow shading. Red curve represents failure just at the wellbore wall, fracture gradient (light blue curve), breakdown (dark blue), mud weight used for drilling (dashed line)
- **Track 9:** Predicted hole instability based on model and mud weight used
- **Track 10:** Bit size and Calipers;

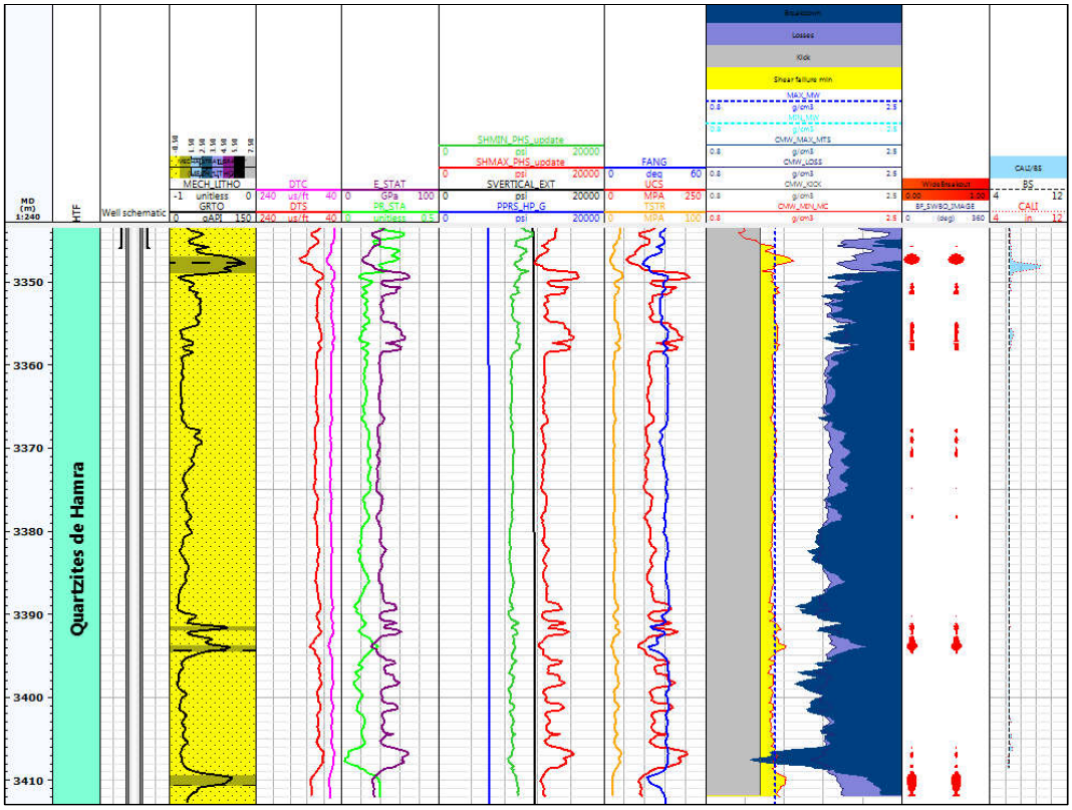

Figure 40: Wellbore stability analysis results for HTF-19

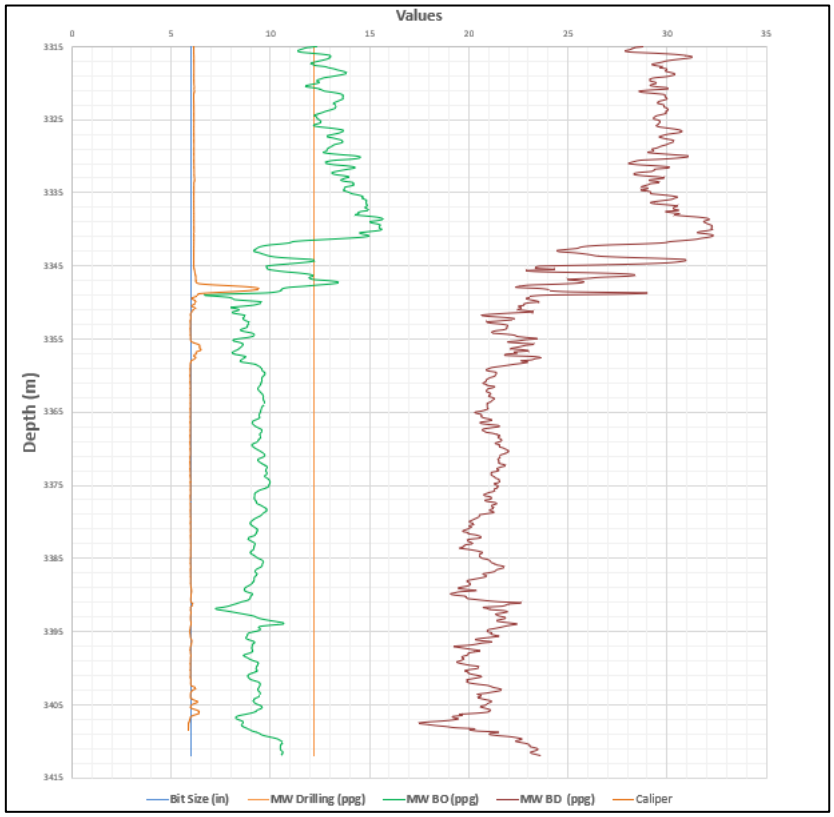

Figure 41: Wellbore stability analysis results for HTF-19 | (Using Excel)

The wellbore of HTF-19 was drilled without causing significant damage, except for some shallow breakouts identified in the Caliper (see Figure 40). The stress regime within the study interval of this well is clearly strike-slip. Moreover, stress anisotropy around HTF-19 is higher compared to other instances. It's noteworthy that the well was drilled with a mud weight of 1.4 sg, which appears suitable for this section.

VI. Conclusions and recommendations

Plans are in place to initiate a hydraulic fracturing campaign targeting the tight formations of the Hamra Quartzite in the Hassi Tarfa field. This study aims to evaluate mechanical the formation properties and in-situ stresses crucial for fracturing design. The analysis involved 1D Geomechanical modeling of HTF-19 well, with the following findings summarized:

Preliminary work entailed collecting analyzing and organizing data, including:

- Well logs (sonic, density, gamma ray, and Caliper) for HTF-19.
- Formation pressure data from borehole tests.
- Mechanical lab tests on cores from HTF-19 and HTF-10. HTF-10 was included due to its coverage of the same formations as the studied well and provision of additional core tests necessary for mechanical properties evaluation.
- Fracturing reports.
- Drilling reports

Using wireline logs, rock properties of the Hamra Quartzite were calculated and calibrated with mechanical lab tests. Confined and unconfined rock properties indicate that the Hamra Quartzite is not highly sensitive to stress. Elastic properties calculations suggest Young's modulus ranging from 40 to 60 GPa and a Poisson's ratio around 0.12. These calculations imply that horizontal stress profiles are more closely associated with Young's modulus than with Poisson's ratio. The Young's modulus profiles show a noticeable increase towards the top of the Hamra Quartzite, just below the casing shoes in the well.

Rock strength properties were also calculated and calibrated using mechanical core tests on plugs and scratch tests. A nearly linear correlation was established between Young's modulus and UCS, aiding in UCS calculation. UCS calculations show that UCS in the sandstones of the Hamra Quartzite ranges from 100 to locally 200 MPa, consistent with UCS measured by scratch tests. According to the Deere and Miller classification (1956) of intact rock strength, Hamra Quartzite sandstones in Hassi Tarfa fall within the medium to strong formations domain. A ratio of 6% of UCS is applied to calculate the tensile strength.

The observed stress regime for the well is predominantly Strike-Slip ($\sigma_H > \sigma_V > \sigma_h$) along the Hamra Quartzite. The minimum stress profile in the reservoir section indicates a potential barrier for hydraulic fracturing, more pronounced at the top of the reservoir than in its lower part. The combination of stresses around the well, coupled with high Young's modulus, complicates the stimulation of the Hamra Quartzite but does not render it impossible. However, conclusions regarding potential containment are solely based on the stress profile and need validation in the stimulation design.

A reasonable match between simulated and observed rock failure is achieved after conducting wellbore stability analysis for the selected well. Limited rock failure intervals were observed in areas dominated by shear failure.

Based on sensitivity analysis on wellbore trajectory, drilling deviated wells in HTF Hamra Quartzite appears to be not highly challenging. One final simulation was

conducted to analyze the impact of depletion on formation stability if open-hole completion is adopted. Different scenarios indicate that during depletion, the Hamra Quartzite may not sustain shear failure under production conditions.

For drilling considerations, the suitable mud weight density for the section of Hamra Quartzite is around 1.4 S.G.

The MEM built and well calibrated for the well HTF-19, with high data and results quality, could potentially be used for further geomechanics modelling of offset and future wells, especially for drilling and fracturing purposes.

Chapter IV: Results and Discussion

Chapter IV: Results and Discussion

I. Introduction

Understanding stress regimes and wellbore stability is crucial for efficient drilling and hydraulic fracturing. This section examines the HTF19 well, focusing on stress interpretation and wellbore stability to optimize drilling and ensure safety. Key parameters include vertical stress, maximum and minimum horizontal stresses, and closure pressure. Additionally, mud weight analysis is essential for maintaining wellbore integrity. The findings offer valuable insights for improving drilling and fracturing operations.

II. Stress interpretation

Normal Regime

In this stress regime, the vertical stress (σ_v) is the greatest principal stress. The order of stress magnitudes is such that the vertical stress is greater than both the maximum horizontal stress (σ_H) and the minimum horizontal stress (σ_h).

Equation: $\sigma_v > \sigma_H > \sigma_h$

Strike-slip Regime

In this stress regime, the maximum horizontal stress (σ_H) is the greatest principal stress, and the minimum horizontal stress (σ_h) is the least principal stress. The order of stress magnitudes is such that the maximum horizontal stress is greater than the vertical stress (σ_v), which in turn is greater than the minimum horizontal stress.

Equation: $\sigma_H > \sigma_v > \sigma_h$

Reverse Regime

In this stress regime, the vertical stress (σ_v) is the least principal stress. The order of stress magnitudes is such that both the maximum horizontal stress (σ_H) and the minimum horizontal stress (σ_h) are greater than the vertical stress.

Equation: $\sigma_H > \sigma_h > \sigma_h$[15]

[15] Effects of different stress regimes on hydraulic fracture geometry: a particle flow code approach" by Sajjad Jalili and Kaveh Ahangari, published in Innov. Infrastruct. Solut. in 2017.

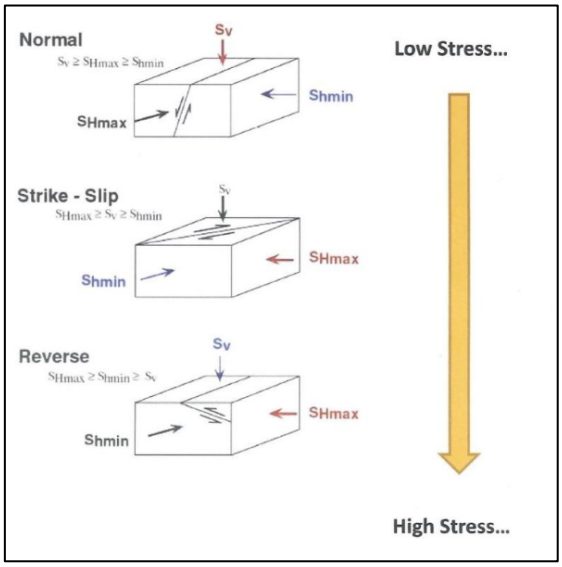

Figure 42: Stress Regime

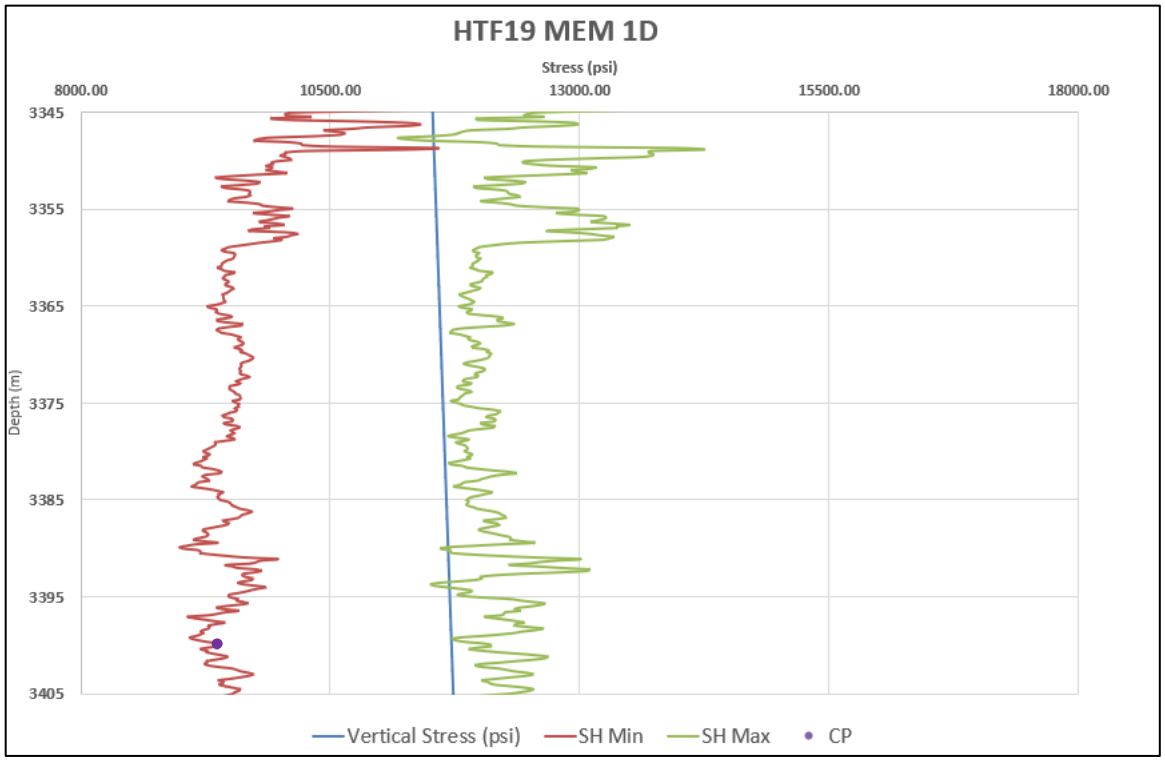

Figure 43: HTF19 MEM 1D Stress Profile Log (By Excel)

- Closure Pressure (CP - **Purple Point**): The pressure at which artificially induced fractures begin to close, critical for hydraulic fracturing design. The CP value is 9,367 psi.

II.1 Vertical Stress Analysis

The vertical stress increases from approximately 8,000 psi at 3,335 feet to around 18,000 psi at 3,405 feet. This trend is indicative of normal geological compaction and aligns with the expected overburden pressure due to the weight of the overlying rock strata.

Closure Pressure (CP) Consideration
Marked by a purple point on the graph, the closure pressure (CP) is 9,367 psi. CP is a pivotal parameter for hydraulic fracturing design, indicating the pressure at which artificially induced fractures begin to close. This informs the necessary pressures for effective fracture propagation.

NB: Good considerations: Implications of Vertical Stress Proximity to SH min

The proximity of vertical stress to SH min suggests a strike-slip faulting stress regime.

- Advantages: This condition can be advantageous for hydraulic fracturing, as it may lower the pressure required to initiate and propagate fractures, leading to more efficient operations.
- Risks: However, if vertical stress and SH min are too closely aligned, there could be increased risks of unintentional fracturing or wellbore instability during drilling.

Therefore, integrating this data with other geomechanical information is crucial to ensure safe and effective reservoir exploitation.

The HTF19 MEM 1D Stress Profile indicates a subsurface environment characterized by steadily increasing vertical stress, significant horizontal stress variation, and a key calibration point provided by the closure pressure of 9,367 psi. These insights are essential for optimizing drilling strategies, designing successful hydraulic fracturing programs, and maintaining operational safety during reservoir development.

III. Mud Weight

- **MW Drilling**: This line represents the actual mud weight used during drilling operations. It should ideally be within the safe window between MW BO and MW BD to prevent wellbore instability.
- **MW BO:** The Mud Weight Breakout indicates the lower threshold of mud weight. If the actual mud weight falls below this line, there's a risk of the wellbore walls fracturing or "breaking out," which can lead to complications such as stuck pipe or loss of well integrity.
- **MW BD:** The Mud Weight Breakdown represents the upper threshold of mud weight. Exceeding this limit can cause a breakdown or loss of circulation due to formation fluids entering the wellbore, which can result in a blowout if not controlled.

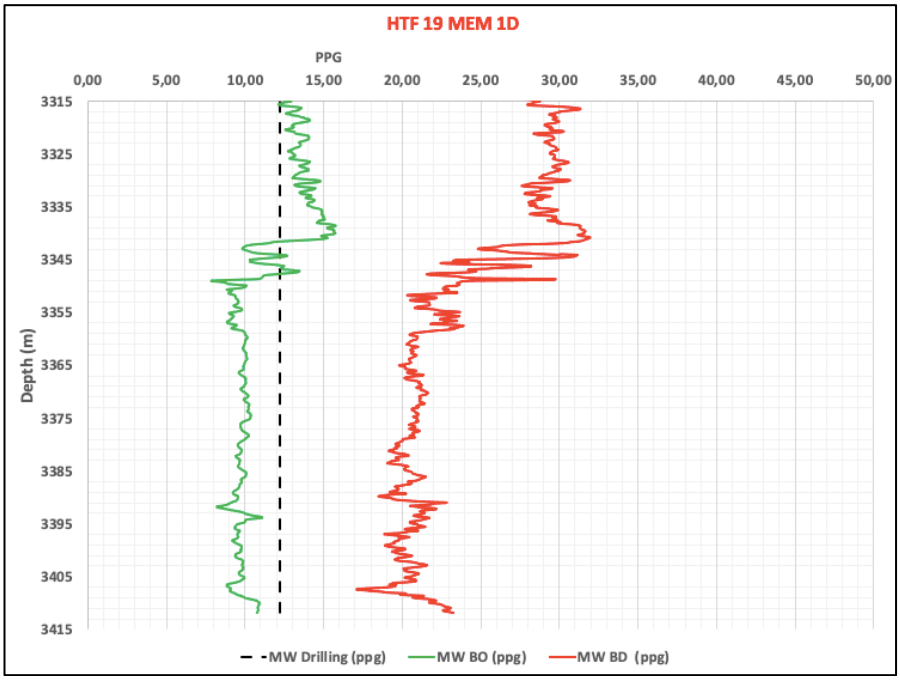

Figure 44: Wellbore stability analysis results for HTF-19

1. **Upper Section (3315m - 3335m):**
    - Narrow, with MW BO at 12-14 PPG and MW BD at 25-27 PPG.
    - This section shows a typical stability window for the initial drilling phase. The mud weight should be maintained around 15 PPG to prevent both breakouts and breakdowns. This phase change doesn't indicate formation instability but reflects the transition between different drilling phases.
2. **Middle Section (3335m - 3385m):**
    - Broader compared to the upper section, with MW BO at 08-16 PPG and MW BD at 19-32 PPG.
    - This range offers a relatively stable drilling window. Maintaining a mud weight of around 15 PPG should ensure safe operations. The increased tolerance provides more flexibility in managing wellbore stability.
3. **Lower Section (3385m - 3415m):**
    - Variable and narrower due to fluctuations in MW BD, which peaks up to 23 PPG.
    - This section presents a more challenging drilling environment. The mud weight should be carefully adjusted, ideally remaining around 15 PPG, but vigilance is necessary due to the potential for sudden changes in formation pressure.

Comparison of the bit size and wellbore size

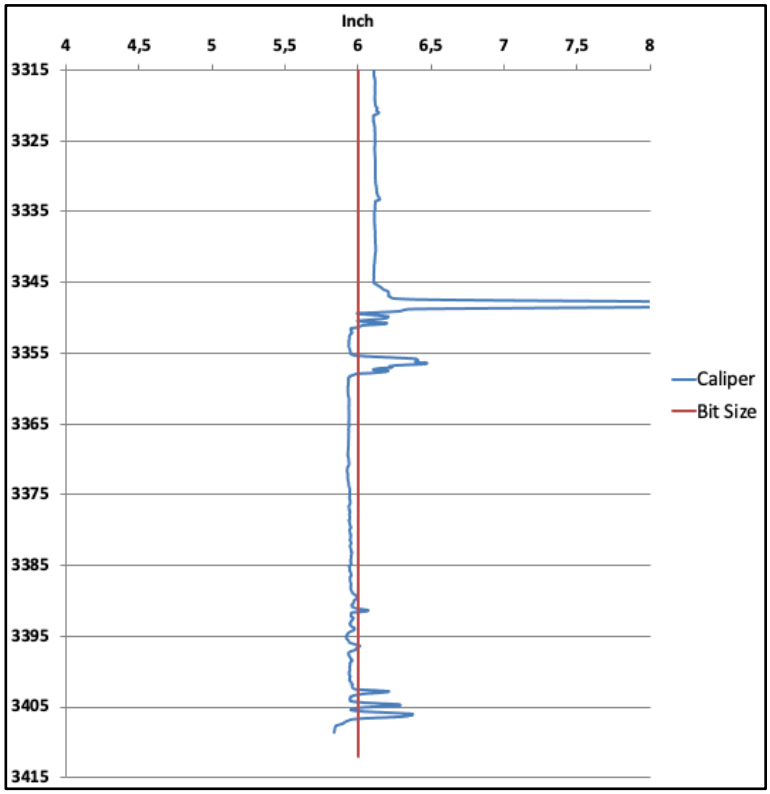

Figure 45: Comparing Wellbore to Bit Size Diameter: Stability Assessment (Using Excel)

1. **Upper Section (Stable Drilling Phase):**

   In the upper section of the plot (around depths 3315 to 3345 m), we observe slightly deviation between the caliper and bit size lines which indicates a good hole and stable wellbore. The wellbore closely matches the 6-inch bit size during this phase; the hole just slightly bigger than the bit.

2. **Medium Section (Instable Drilling Phase):**

   In the upper section of the plot (around depths 3345 to 3360 m), we observe important local deviation between the caliper and bit size lines which indicates a bad hole and instable wellbore. In two locations, the wellbore doesn't match the 6-inch bit size during this phase; the hole is significantly bigger than the bit.

3. **Lower Section (Stable Drilling Phase):**

   In the lower section of the plot (around depths 3360 to 3415 m), we observe slightly deviation between the caliper and bit size lines which indicates a good hole and stable wellbore. The wellbore closely matches the 6-inch bit size during this phase; the hole just slightly smaller than the bit.

It seems that drilling the well with a mud weight equal to 12 PPG develop a local instability in this phase, especially between the depth interval 3345-3360 m.

4 Implications:

- Investigate the reasons behind the instability observed in the upper section. Geological formations, drilling conditions, or other factors may contribute.
- In the stable phase, maintaining alignment between caliper and bit size is crucial for overall wellbore integrity.

III.1 Recommended Mud Weight for Drilling a New Well:

Based on the analysis of the wellbore stability and the stability assessment (using caliper data), it is recommended to maintain a mud weight of approximately 15 PPG to ensure safe and efficient drilling operations in the same region (Figure 46).

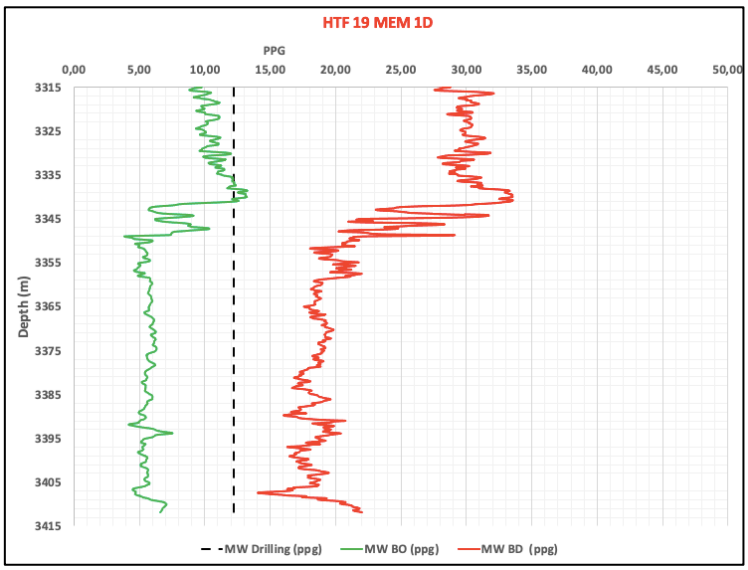

Figure 46: Mud window for new well in HTF region

IV. Conclusion

The HTF19 well exhibits a strike-slip stress regime, with vertical stress close. This condition aids hydraulic fracturing but also risks wellbore instability. The detailed stress and closure pressure analyses provide a comprehensive view of the subsurface environment. Wellbore stability analysis emphasizes the need for appropriate mud weight to prevent collapse or fluid loss. Integrating these insights with other geomechanical data is essential for safe and effective reservoir development.

General Conclusion

The development of a precise 1D Mechanical Earth Model (MEM) represents a significant advancement in the field of petroleum geology, particularly for the exploitation of tight reservoirs. Through the case study of HTF-19, this work has demonstrated the practical applications and benefits of MEM in drilling and hydraulic fracturing operations. By integrating geological, geophysical, and engineering data, the MEM provides a robust framework for understanding the subsurface's mechanical behavior, which is essential for optimizing extraction processes.

The application of MEM in the HTF-19 well has shown that a well-constructed mechanical model can significantly enhance the efficiency and safety of hydrocarbon extraction. For drilling operations, the MEM allowed for precise predictions of pore pressure and stress distribution, which are critical for designing appropriate mud weights and casing programs. This led to improved wellbore stability, reduced risks of wellbore collapse, and minimized incidents of lost circulation and differential sticking. As a result, the drilling process became more efficient and cost-effective.

In addition to drilling, the MEM also facilitated the design of effective hydraulic fracturing treatments. The insights gained from the MEM ensured optimal fracture propagation and improved fluid flow, maximizing hydrocarbon recovery from tight reservoirs. The integration of MEM into the workflow of both drilling and fracturing operations offers substantial economic and operational benefits. It enables more accurate predictions of subsurface behavior, facilitates better decision-making, and ultimately leads to more efficient resource extraction.

Overall, this study underscores the importance of advanced modeling techniques in overcoming the challenges posed by tight reservoirs. The MEM serves as a valuable tool for enhancing both drilling and fracturing operations, highlighting the potential for further innovations in this field. The successful application of MEM in the HTF-19 well exemplifies how a comprehensive understanding of subsurface mechanics can lead to safer, more efficient, and more productive hydrocarbon extraction practices

References

- M. B. a. A. Hamid, “Pore Pressure Prediction in Shale Gas Field,”, March.
- R. Ismail, drilling engineering, Malaysia, 2011.
- G. M. a. A. N. J. Dvorkin, “Overpressure detection from compressional- and shear-wave data,” Geophys. Res. Lett., vol. 26, no. 22, pp. 3417–3420,, 1999.
- Overburden Pressure: What is it and Why is it important? – Top Dog Engineer.
- H. (Rabia, Well Engineering & Construction, London, 2002.
- H. (Rabia, Well Engineering & Construction, London, 2002.
- N. Adams, Drilling Engineering, Tulsa, Oklahoma: Penn well publishing company, 1985.
- G. Z. H. W. D. H. N. a. T. J. Z. Liu, "“Pore characteristics and formation mechanism of high-maturity organic-rich shale in Lower Cambrian Jiumenchong Formation, southern Guizhou,”," vol. 3 - 2018.
- N. Adams, Drilling Engineering, Tulsa, Oklahoma: Penn well publishing company, 1985
- SLB WebSite : https://www.slb.com/resource-library/oilfield-review/defining-series/defining-mem
- SLB website : https://glossary.slb.com/en/terms/b/breakdown_pressure
- Society of Petroleum Engineers (SPE). (2007). *Petroleum Engineering Handbook: Volume II - Drilling Engineering*. Richardson, TX: Society of Petroleum Engineers.
- Effects of different stress regimes on hydraulic fracture geometry: a particle flow code approach" by Sajjad Jalili and Kaveh Ahangari, published in Innov. Infrastruct. Solut. in 2017.
- 1D Geomechanics modelling for hydraulic fracturing design in Hassi Tarfa field (SLB - SIS-Data Services)